Deanship of Graduate Studies

Al-Quds University

Complexes formed between polyelectrolyte and acetylated cationic dendrimers.

Raghad Abdalmuiz Daoud Natsha

M.Sc. Thesis

Jerusalem – Palestine

1444/2022

Complexes formed between polyelectrolyte and modified cationic dendrimers

Prepared by:

Raghad Abdalmuiz Daoud Natsha

B.Sc. Chemistry, and a minor Chemical Technology. Al-Quds University. Palestine.

Supervisor: Dr. Khawla Qamhieh

A Thesis Submitted in partial fulfilment of requirements for the degree of Master of Chemical Industry in Applied and Industrial Technology Program. Al-Quds University

1444/2022

Al-Quds University

Deanship of Graduate Studies

Applied and Industrial Technology program

Thesis approval

Complexes formed between polyelectrolyte and modified cationic dendrimers

Prepared by: Raghad Abdalmuiz Daoud Natsha

Registration No: 21812459

Supervisor: Dr. Khawla Qamhieh

Master thesis Submitted and Accepted, Date: 17/12/2022

The name and signature of examining committee member are as follows:

1- Head of Committee:	Dr. khawla qamhieh	Signature:
2- Internal Examiner:	Dr. Wadie Sultan	Signature:
3- External Examiner:	Dr. Jamal Ghabboun	Signature:

Jerusalem – Palestine

1444/2022

Dedication

I dedicate this study to those who have the dream of completing their education but can't; poor people, refugees, Palestinian prisoners, and all Palestinians in the Diaspora.

Declaration

I declare that my thesis is based on findings I made on my own. Work and results found by other researchers are documented and cited. This thesis, neither in whole or in part, has been previously submitted for any educational degree. The study was performed under the supervision of Dr. Khawla Qamhieh, at Al – Quds University, Jerusalem, Palestine.

Name: Raghad Abdalmuiz Daoud Natsha

Signed: 

Date: 17/12/2022

Acknowledgment

First and foremost, we express gratitude to Allah the Almighty.

I would like to thank my supervisor Dr. Khawla Qamhieh, for her professional advice, valuable guidance, and hard efforts in completing this project.

I would like to thank my siter Dr. Zahra Natsha, for her help in editing this thesis.

I am also grateful to everyone who encouraged me during my studies, including my family, friends, work colleagues, and professors.

Abstract

Gene therapy has received a lot of attention over the past two decades since research efforts are presently concentrated on developing effective carrier vectors for gene therapy that effectively condense and preserve deoxyribonucleic acid (DNA). The complexation of negatively charged linear polyelectrolyte chain (LPE) and acetylated dendrimer has been investigated using the penetrable sphere model developed by Qamhieh et al. describing the interaction between linear polyelectrolyte (LPE) chain and ion-penetrable. In this research, we examined the effects of two factors on the complexes formed: the acetylation percentage of the dendrimer and the length of the LPE chain. The complexes formed by the poly (amido amine) (PAMAM) dendrimer of generation 5 and (DNA) are studied for three different DNA lengths: L = 90 nm of 265; L = 184 nm of 541 bp; and L = 680 nm of 2000 bp. As a result, for polyelectrolyte (PE) – single dendrimer complexes, as the acetylation percentage increases, the ratio of optimal length to the length of LPE and condensed monomers around the acetylated dendrimer decreased. Also, by increasing the acetylation percentage, the complexes with lengths of 90 nm for both single strand-DNA and double strand-DNA, have negative net charges, which get more negative as dendrimer radius decreases. For the length of 184 nm from 30% to 100% acetylation, and for the length of 680 nm from 0% to 90% acetylation, in the case of ssDNA and dsDNA, the net charge is negative and decreases in negativity. For PE – two dendrimer complexes, the net charge of the complexes with lengths of 90 and 184 nm of both ssDNA and dsDNA is negative and increases in negativity by increasing acetylation. For the complexes using a length of 680 nm, in the case of ssDNA and dsDNA, it was shown that the net charge of the complexes decreased in its negative charge by increasing acetylation. For these two types of complexes, the optimal length of all used lengths, decreases significantly with increasing acetylation. While the number of turns of the ss and ds LPE chains with a length of 680 nm around the acetylated dendrimer decreased considerably, the number of turns of the shorter 90 and 184 nm for both single strand and double strand LPE chains remained relatively constant. For a system with multiple dendrimers, at different acetylation percentages, the optimal length decreases with increasing acetylation, which in turn increases the linker length. While at zero-acetylation percentage, the ratio of optimal length wrapping around the dendrimer to the length of LPE decreases as the chain length increases, while the optimal length, the linker length, the condensed monomers, and the number of turns around the dendrimer increase with increasing LPE chain

length. These factors' impact on complex formation varies depending on the dendrimer's radius, charge, and core type (ammonia or ethylenediamine cored dendrimers). In this study, it is demonstrated that the created model is fit for explaining the complexation between the LPE and the dendrimer.

List of Contents

Content	Page No.
Declaration	i
Acknowledgements	ii
Abstract	iii
Table of contents	v
List of tables	vii
List of figures	ix
List of abbreviations	xii
Chapter One: Introduction	
1.1 Introduction	2
1.2 Gene therapy	3
1.3 Polyelectrolyte	4
1.3.1 Applications of PECs	7
1.3.2 Types of PECs	7
1.3.3 Characterization of PECs	8
1.3.4 DNA	8
1.4 Dendrimers	9
1.4.1 Dendrimer structure	9
1.4.2 Dendrimer properties	10
1.4.3 Dendrimer synthesis	11
1.4.3.1 Divergent method	11
1.4.3.2 Convergent method	12
1.4.4 Dendrimer cytotoxicity	13
1.4.5 PAMAM dendrimers	14
1.4.6 Application of PAMAM in DNA	15
1.5 Modified dendrimers	18
1.5.1 Effect of acetylation	21
1.6 Charge Inversion (overcharging)	23
1.7 Polyelectrolyte/dendrimer complexation	23
1.8 Effect of salt on complexation.	24
1.9 Literature survey	26
1.10 Statement of the problem and the Objectives	30
Chapter Two: Model and Methods	

2.1 Introduction 32
2.2 Complexation of a LPE chain with a single sphere 32
2.3 Calculation of the free energy for the dendrimer/DNA aggregate 35
2.4 Software Analysis 37

Chapter Three: Results and Discussion

3.1 Introduction 39
3.2 Computational details 39
3.3 Single PAMAM dendrimer – LPE chain complex 40
3.3.1 Effect of Acetylation on single PAMAM– LPE chain complexes 40
3.4 System of multiple PAMAM dendrimers – LPE chain complexes 49
3.4.1 Effect of Acetylation on multiple PAMAM dendrimer – LPE complex conformation. 49
3.4.2 Effect of LPE chain length on the zero acetylated dendrimer - LPE complex. 63

Chapter Four

Conclusion 70
References 72
الملخص 79

List of Tables

Table	Title	Page No.
Table 1.1	Charge and radius of PAMAM generations as provided from the manufacturer, Dendritech. While surface charge density was calculated in this study.	11
Table 1.2	Illustrates modified PAMAM dendrimers with different generations, molecular weights and end groups.	19
Table 3.1	Properties of the PAMAM dendrimer (EDA) core of different radii, R_s, investigated by (Shi Yu, 2015), while the charge of the acetylated dendrimer Z_d, the surface charge density σ and the isoelectric length l_{iso} have been investigated by this study.	40
Table 3.2	The amount of radius R_s and charge Z_d reduction caused by acetylation.	40
Table 3.3	The interaction between acetylated G5 dendrimer N=1 and LPE of chain length L = 90 nm, with ss when b=0.34 nm.	43
Table 3.4	The interaction between acetylated G5 dendrimer N=1 and LPE of chain length L = 90 nm, with ds when b=0.17 nm.	43
Table 3.5	The interaction between acetylated G5 dendrimer N=1 and LPE of chain length L = 184 nm, with ss when b=0.34 nm.	43
Table 3.6	The interaction between acetylated G5 dendrimer N=1 and LPE of chain length L = 184 nm, with ds when b=0.17 nm.	44
Table 3.7	The interaction between acetylated G5 dendrimer N=1 and LPE of chain length L = 680 nm, with ss when b=0.34 nm.	44

Table 3.8	The interaction between acetylated G5 dendrimer N=1 and LPE of chain length L = 680 nm, with ds when b=0.17 nm.	44
Table 3.9	The interaction between acetylated G5 dendrimers N=2 and LPE of chain length L = 90 nm, with ss when b=0.34 nm.	53
Table 3.10	The interaction between acetylated G5 dendrimers N=2 and LPE of chain length L = 90 nm, with ds when b=0.17 nm.	53
Table 3.11	The interaction between acetylated G5 dendrimers N=2 and LPE of chain length L = 184 nm, with ss when b=0.34 nm.	54
Table 3.12	The interaction between acetylated G5 dendrimers N=2 and LPE of chain length L = 184 nm, with ds when b=0.17 nm.	54
Table 3.13	The interaction between acetylated G5 dendrimers N=2 and LPE of chain length L = 680 nm, with ss when b=0.34 nm.	54
Table 3.14	The interaction between acetylated G5 dendrimers N=2 and LPE of chain length L = 680 nm, with ds when b=0.17 nm.	55

List of Figures

Figure	Title	Page No.
Figure 1.1	Schematic representation of (a) a piece of a DNA molecule is shown to wrap around one dendrimer. The DNA segments linking to the next dendrimer in an aggregate. (b) a dendrimer/DNA complex consisting only of one dendrimer and the DNA segment actually wrapping the dendrimer, l. (c) the dendrimer/DNA aggregate consisting of the entire DNA molecule and a multiple of dendrimers (Qamhieh et al., 2014).	3
Figure 1.2	Steps of DNA complexation toward the cell in gene therapy. (lipolexes).	4
Figure 1.3	Dissociation of (a) a simple electrolyte and (b) a polyelectrolyte in an aqueous solution.	5
Figure 1.4	DNA structures.	9
Figure 1.5	Dendrimer structure (Janaszewska, A. et al., 2019)	10
Figure 1.6	Synthesis of dendrimers by the divergent growth method (Santos, A. et al., 2019).	12
Figure 1.7	Synthesis of dendrimers by the convergent growth method (Santos, A. et al., 2019).	13
Figure 1.8	The effect of the surface charge of dendrimers on their bioavailability, immunogenicity, and in vitro and in vivo toxicity. "+" indicates that there is an effect; "−" indicates no effect. (Santos, A. et al., 2019).	14
Figure 1.9	Generation 2 PAMAM Dendrimer (for larger view).	17
Figure 1.10	Dendrimer Terminal Group (for larger view).	17
Figure 1.11	Acetylation of PAMAM dendrimer.	18
Figure 1.12	Snapshots at the beginning (0 ns, top images) and end (4.9 ns for G5, 4.5 ns for G5M, 6.4 ns for G5-Ac90, and 5.0 ns	22

	for G5M-Ac90, bottom images) of (a) G5, (b) G5M, (c) G5-Ac90, and (d) G5M-Ac90 simulations. Protonated surface residues (NH3 +) are shown as blue dots. The explicit water molecules and counterions are omitted for clarity. The images ware created using VMD (Humphrey, W. et al., 1996).	
Figure 1.13	Negatively charged DNA with positively charged PAMAM dendrimer.	23
Figure 1.14	The optimal spatial configuration of the complex fiber, for macroion (sphere) charge valency Z = 15, total chain length per unit cell (per sphere) of Lc = 68 nm (equivalent to 200 DNA base pairs) and for various Debye inverse screening lengths as indicated on the graph. (Boroudjerdi, H., et al., 2011).	25
Figure 3.1	The ratio of l_{opt} to the length of PE as a function of acetylation %. (Solid lines for ss, dashed lines for ds).	41
Figure 3.2	The number of condensed monomers as a function of acetylation %. (Solid lines for ss, dashed lines for ds).	42
Figure 3.3	l_{opt} as a function of acetylation %, when N=1. (Solid lines for ss chains, and dashed lines for ds chains).	48
Figure 3.4	The net charge of the complex Z^* ($Z_{complex}$) as a function of acetylation %. (Solid lines for ss chains, and dashed lines for ds chains).	48
Figure 3.5	Number of turns on the dendrimer around LPE chain as a function of acetylation %. (Solid lines for ss chains, and dashed lines for ds chains).	49
Figure 3.6	l_{opt} and Linker formed between G5 complexes with an oppositely charged semiflexible LPE as a function of acetylation %. The LPE chain length used, L=184 nm. (a) and (c) for ss b=0.34, (b) and (d) for ds b=0.17.	51
Figure 3.7	l_{opt} and Linker formed between G5 complexes with an oppositely charged semiflexible LPE as a function of acetylation %. The LPE chain length used, L=680 79nm. (a) and (c) for ss b=0.34, (b) and (d) for ds b=0.17.	52
Figure 3.8	l_{opt} a function of acetylation %, when N=2. (Solid lines for ss chains, and dashed lines for ds chains).	58

Figure 3.9	The net charge of the complex Z^* ($Z_{complex}$) as a function of acetylation %. (Solid lines for ss chains, and dashed lines for ds chains).	59
Figure 3.10	Number of turns on the dendrimer around LPE chain as a function of acetylation %. (Solid lines for ss chains, and dashed lines for ds chains).	59
Figure 3.11	The net charge of the complex Z^* ($Z_{complex}$) as a function of acetylation %. (a) for N=3, (b) for N=4, (c) for N=5, and (d) for N=6. When L = 184 nm and L = 680 nm. Solid lines for ss chains, and dashed lines for ds chains.	60
Figure 3.12	Number of turns of LPE chain on the dendrimer as a function of acetylation %. (a) for N=3, (b) for N=4, (c) for N=5, and (d) for N=6. When L = 184 nm and L = 680 nm. Solid lines for ss chains, and dashed lines for ds chains.	61
Figure 3.13	Number of turns of LPE chain on the dendrimer at zero % acetylation, when N=2, 3, 4, 5, and 6 and L=680 nm as a ds chain.	62
Figure 3.14	Number of turns of LPE chain on the dendrimer at 40 % acetylation, when N=2, 3, 4, 5, and 6 and L=680 nm as a ds chain.	62
Figure 3.15	Number of turns of LPE chain on the dendrimer at 90 % acetylation, when N=2, 3, 4, 5, and 6 and L=680 nm as a ds chain.	63
Figure 3.16	l_{opt} and Linker formed between G5 complexes with an oppositely charged flexible LPE as a function of chain length L. (a) For optimal length, (b) for linker formed between G5 complexes. Dashed lines for EDA core and solid lines for ammonia core.	64
Figure 3.17	The ratio of l_{opt} as a function of PE chain length L. (a) For EDA core (dashed lines), (b) for ammonia core (solid lines).	66
Figure 3.18	(a)The number of condensed monomers as a function of PE chain length (b) the number of turns warp around dendrimer as a function of PE chain length L. Dashed lines for EDA core, and solid lines for ammonia core.	68

List of Abbreviations

DNA	Deoxyribonucleic acid
RNA	Ribonucleic acid
LPE	Linear Polyelectrolyte
PAMAM	Poly(amido amine)
N	Number of dendrimer particles
Z_d	Charge of dendrimer
EDA	Ethylenediamine
NMR	Nuclear Magnetic Resonance
MD	Molecular Dynamic
BD	Brownian Dynamic
Rg	Radius of gyration
Rs	Radius of sphere
Bp	base – pair
l_{opt}	The optimal wrapping length of chain around dendrimer
l_{iso}	The length of the chain needed to neutralized the charge of dendrimer
DLS	Dynamic light scattering
lp	The persistence length of LPE chain
lB	Bjerum length
AFM	Atomic Force Microscopy
Ds	Double strand
Ss	Single strand
Ac	Acetylated

Chapter One

Introduction

1.1 Introduction

It is important to develop and study new applications and various approaches to find pivotal and effective ways for the treatment of many diseases in human bodies, one of these ways is to develop a system composed of DNA, as a polyelectrolyte wrapping around dendrimer. These complexes can penetrate cell membranes which have a great potential for gene delivery. The application of dendrimers as nonviral vectors is considered a fundamental approach in the field of nano-medicine for drug delivery and gene therapy. Gene therapy gained its name from the use of genetic material in altering gene expression within a specific cell population, thus changing the processes within the cell (Scheller, E. L et al., 2009).

At present, the development of dendrimer/polyelectrolyte complexes (dendriplex), is important for many applications; such as surface coating (dendrimers on gold surface for example) (Wolski et al., 2019) colloid stabilization, paper making, methanol oxidation, optical sensing, fingerprint detection (Jin, Y et al., 2008), and Gene therapy.

The structure of dendriplex Fig. (1.1), can be influenced by many Physico-chemical parameters turned out to be effective and reliable for adjusting the formation of polyelectrolyte/dendrimer complexes to obtain stable conformation. The polyelectrolyte parameters are the contour length (the length of a single strand polyelectrolyte at its maximum extension), the linear charge distribution of the polyelectrolyte, the persistence length (the effective rigidity of the polyelectrolyte) and the linear charge density (Qamhieh et al., 2014). The dendrimers parameters are the size of the dendrimer and the surface charge density of it. Other additional parameters are the ionic strength (effect of salt concentration), pH (which affects the surface charge density), and critical adsorption. The latter one is used in theoretical studies when polyelectrolyte adsorbed onto planar and curved surfaces which introduce and demonstrate a phase-transition behavior (Caetano et al., 2020)

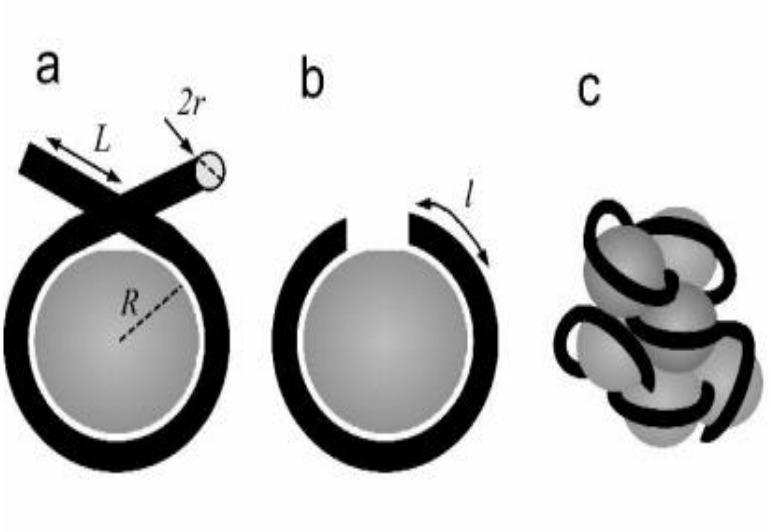

Figure 1.1: Schematic representation of (a) a piece of a DNA molecule is shown to wrap around one dendrimer. The DNA segments linking to the next dendrimer in an aggregate. (b) a dendrimer/DNA complex consisting only of one dendrimer and the DNA segment actually wrapping the dendrimer, l. (c) the dendrimer/DNA aggregate consisting of the entire DNA molecule and a multiple of dendrimers (Qamhieh et al., 2014).

1.2 Gene therapy

Gene therapy works on DNA sequences and various cell types, it applies many methods to obtain enough DNA to access and modify these cells as illustrated in Fig. (1.2), (Pereyra, A et al., 2013). Recently, gene therapy has gained prominence, particularly in the treatment of viral diseases such as coronavirus. However, to correctly apply and verify gene therapy we have to perform gene delivery. Therefore, viral vectors are used to deliver genetic material into the cells. This allows scientists to engineer viruses genetically; an example is using the viral DNA and RNA to produce coronavirus proteins which are used as a vaccine (Abu Abed, 2021). Indeed, this is considered an efficient and reliable way to enhance an immune response. Therefore, Pfizer, a biopharmaceutical company, began to improve vaccines by modifying the nucleic acid and wrapping the ssRNA of spike proteins in lipids. In addition, Moderna's Company vaccines were developed in the same way and are the second vaccines licensed by the FDA one week after Pfizer (Abu Abed, 2021).

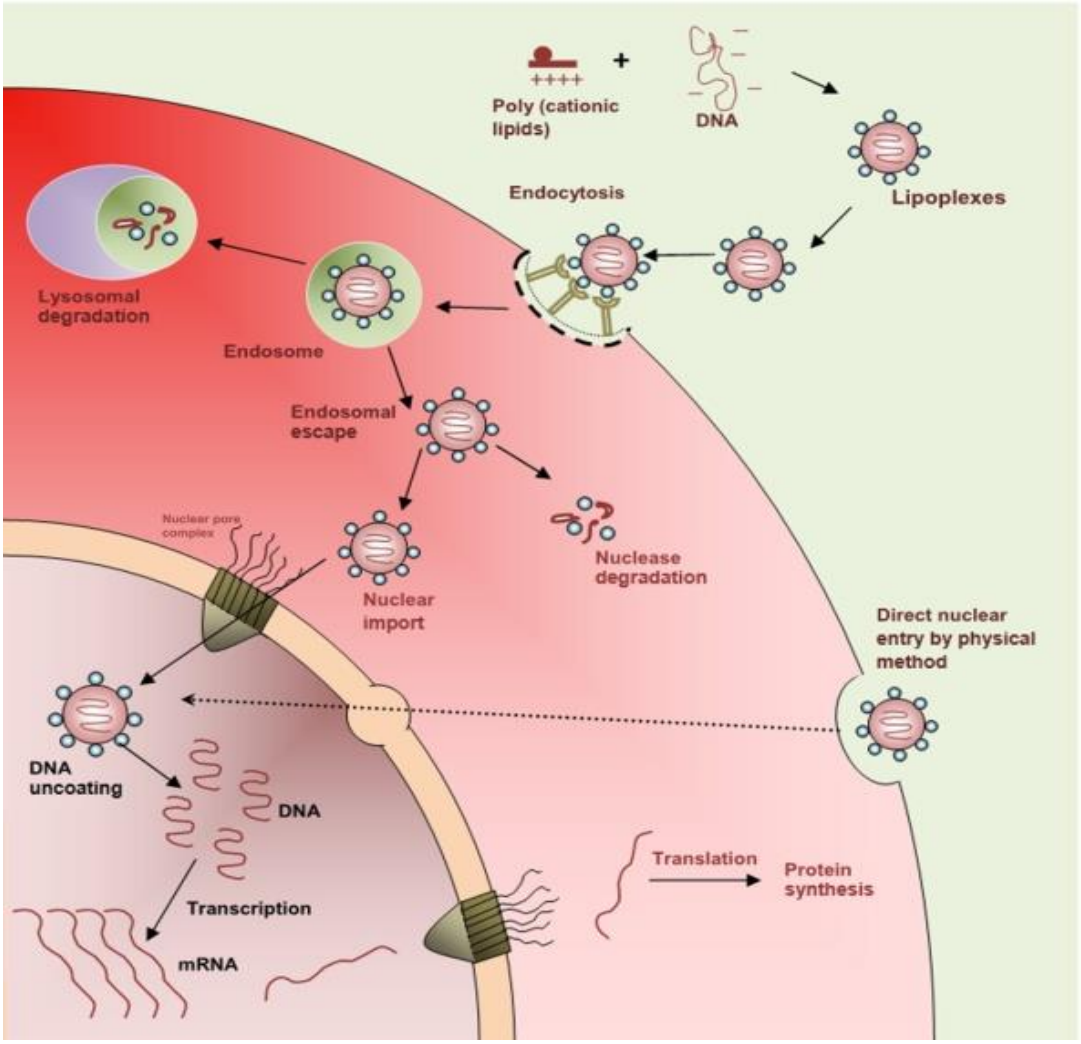

Figure 1.2: Steps of DNA complexation toward the cell in gene therapy. (lipolexes) (Pereyra, A et al., 2013).

1.3 Polyelectrolytes

For decades, polyelectrolytes have been studied for their unique properties, such as flexibility and interactions, which could be used in biological and medical technologies. Polyelectrolytes are macromolecules that have monomers (repeat units) with their own charges it can be positive or negative charges that may be separated when dissolved in water as illustrated in Fig. (1.3). The same is true for NaCl, which has positive and negative charges that can be separated (Dias, R et al., 2008).

The distinction for polyelectrolytes in that either positive or negative charges are combined to produce a highly charged molecule. There are also large charged molecules known as polyampholytes, but they include both types of charges, and can even be electroneutral on the net. The charge distribution of polyelectrolytes and polyampholytes can be classified as either strong (quenched), which is governed entirely by the chemical sequence, or weak (annealed), which has charges that can move inside the molecule and respond to external factors, such as the pH of the solution. In other terms, weak polyelectrolytes are weak polyacids or polybases, with poly (acrylic acid) and poly (vinylamine) as synthetic instances (Dias, R et al., 2008).

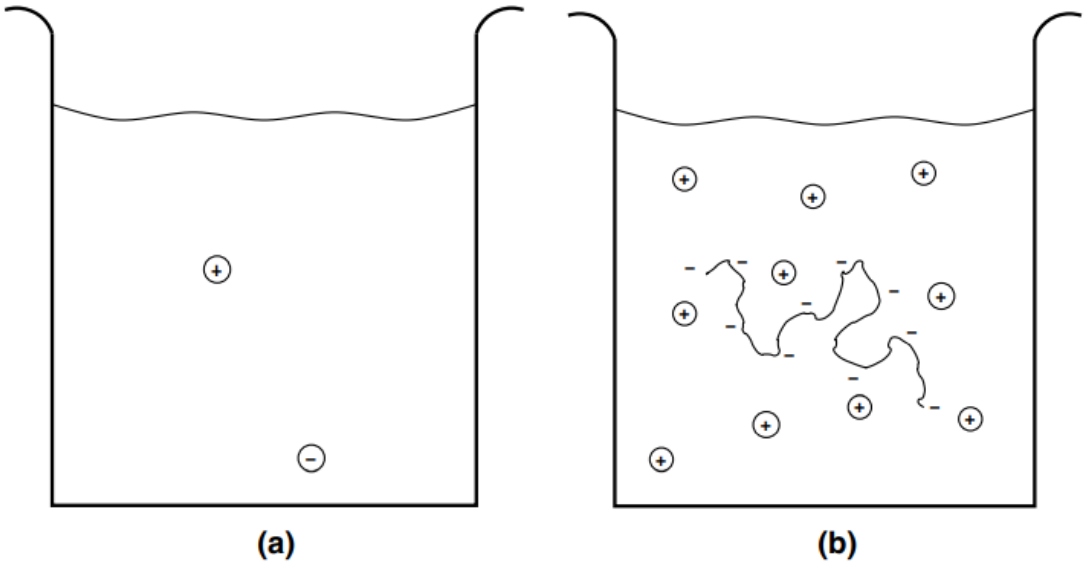

Figure 1.3: Dissociation of (a) a simple electrolyte and (b) a polyelectrolyte in an aqueous solution (Dias, R et al., 2008).

It is no accident that many biomolecules are polyelectrolytes since, at the molecular level, life is made up of several components that must all be water soluble and interact in a predictable way. Proteins, for instance, often include both acidic and basic groups and are polyampholytes, whereas DNA and RNA are strong polyelectrolytes (Dias, R et al., 2008).

Alginates, hyaluronan, and pectin are a few naturally occurring polysaccharides that are also polyelectrolytes. Carrageenans and carboxymethylcellulose are two examples of natural polysaccharides can be modified to produce polyelectrolytes. Technically speaking, a large number of polysaccharides—both charged and non-ionic—are utilized as thickeners, gelling agents, and

emulsion stabilizers (Dias, R et al., 2008). They may do comparable tasks in a biological setting, producing structural viscoelastic components. Hyaluronan, for instance, plays a significant role in the vitreous body of the human eye (Dias, R et al., 2008). Since the polysaccharides are too big to fit within the compartment, once they are charged, the counterions will be held in place to preserve electroneutrality. Water seeks to penetrate the compartment for entropic reasons in order to dilute its contents, and the counterions increase the osmotic impact. The polysaccharide-rich areas of the body have a high water content that results in a gelatinous consistency that may serve as a shock absorbing and lubricating substance in the joints (Dias, R et al., 2008).

Higher biological functions, however, call for a little more than a change in the solution's characteristics. It can be challenging to keep a molecule solubilized in water and prevent aggregation when hydrophobic groups are required to achieve a more precise structure and activity. This is especially true when the larger, more complex molecules are required. By heavily charging these macromolecules, disintegration can be prevented. This promotes solubility by adding a counterion that can independently explore the solution and provide a significant amount of entropy to the dissolved polyelectrolyte, not because by increasing the hydrophilicity of each charged molecule. Entropy increases when counterions increase. The molecule can also be charged to avoid aggregation due to electrostatic repulsion. Entropy increases when counterions increase (Dias, R et al., 2008).

Additionally, charging a molecule can have the desired effect of causing it to aggregate by creating complexes with molecules that have opposite charges, or it can have the inverse effect by preventing aggregation through electrostatic repulsion. The aggregates might be big, like DNA wraps around histone complexes to generate nucleosomes in chromatin, or tiny, like ions attaching to certain locations in proteins (Dias, R et al., 2008).

In solution, polyelectrolytes negative charges neutralized by positively charged ions and vice versa. This is due to the attraction between polyelectrolyte and opposite charged surfaces, which depends on the solution conditions and properties, and the polyelectrolyte charge density which influences the polyelectrolyte behavior. Solution properties such as ionic strength which is considered to be the main property of the solution. At the lower ionic strength of a solution, polyelectrolyte will be in an extended state due to the repulsion forces between its repeating units. But at higher ionic

strength of the solution the polyelectrolyte will change from an extended state to adsorbed and wrapped state. The change in behavior for the polyelectrolyte gives it different sizes and morphologies which increase its use and allow it to be used in many applications, such as the pharmaceutical industry, biomedicine, medicine, water plantation, cosmetics, food, and paper industries (Müller, M., 2013) and etc.

1.3.1 Applications of PEs

Due of the many possible uses of PECs, there has been a lot of interest lately. Because charged particles may readily be incorporated into the complex particles, they also function as medication delivery systems, enzymes, or DNA. These can be used as membranes, film coating, protein isolation and fractionation, targeted nucleic acid delivery, pharmaceutical product binding, creation of microcapsules for drug delivery, dialysis membranes, contact lenses, enzyme mimics, medical applications, nanoparticles for targeted tissue delivery, organelle trafficking and imaging, biosensor development, enzyme immobilization, hydrogels for protein and peptide delivery, and for the treatment of chronobiological illnesses, in developing vaccines for improvement of the immune system's response to antigens (Mok, H., & Park, T. G. et al., 2009; Andrianov, A. K. et al., 2005).

1.3.2 Types of PEC

1. Water-soluble PECs: systems with smaller PEC aggregates that are macroscopically homogeneous (Meka, V. S et al., 2017).
2. Turbid colloidal stable PECs: systems that display in the transition region to phase separation (Dias, R et al., 2008).
3. Complex coacervates or two-phase system PECs: complexes that, after repeated washing and drying, easily separate as solid material (Dias, R et al., 2008).

1.3.3 Characterization of PECs

PECs have been characterized using a variety of techniques. Potentiometric titrations, turbidimetric titrations, differential scanning calorimetry, thermal analysis, ionic strength, pH, weight ratio of polymer in the media, viscosity, gel electrophoresis, static and dynamic light scattering, electron and X-ray absorption microscopy, ultracentrifugation, attenuated total reflectance, scanning electron microscopy , Fourier transform infrared spectroscopy, scanning electron microscopy, atomic force microscopy, powder X-ray diffraction and pKa are methods were used to assess the interpolymer complexation (Müller, M et al., 2002; Reihs, T et al., 2004).

1.3.4 DNA

DNA is a semi-flexible negatively charged polyelectrolyte and can be regarded as a strong polyelectrolyte, this DNA consist of double strands (ds) form a double helix, these double stands are composed of phosphoric acid groups and pentose sugar groups as shown in Fig. (1.4). The interior of the double helix comprises nitrogenous bases, bonded to the sugar groups of the DNA strands, forming the nucleotides, these bases give a negative charge of the backbone of the DNA. The highly negative charge of the DNA gives it an extended form in an aqueous solution due to the repulsion between negatively charged segments, by neutralizing these segments with an addition of oppositely charged species the DNA transit from extended (unfolded) form to a folded form this so-called compaction. The intriguing feature of the DNA chain is its semi-flexible nature which makes it rigid and flexible depending on charge bending and the length of these DNAs (Peters, J. P et al., 2010).

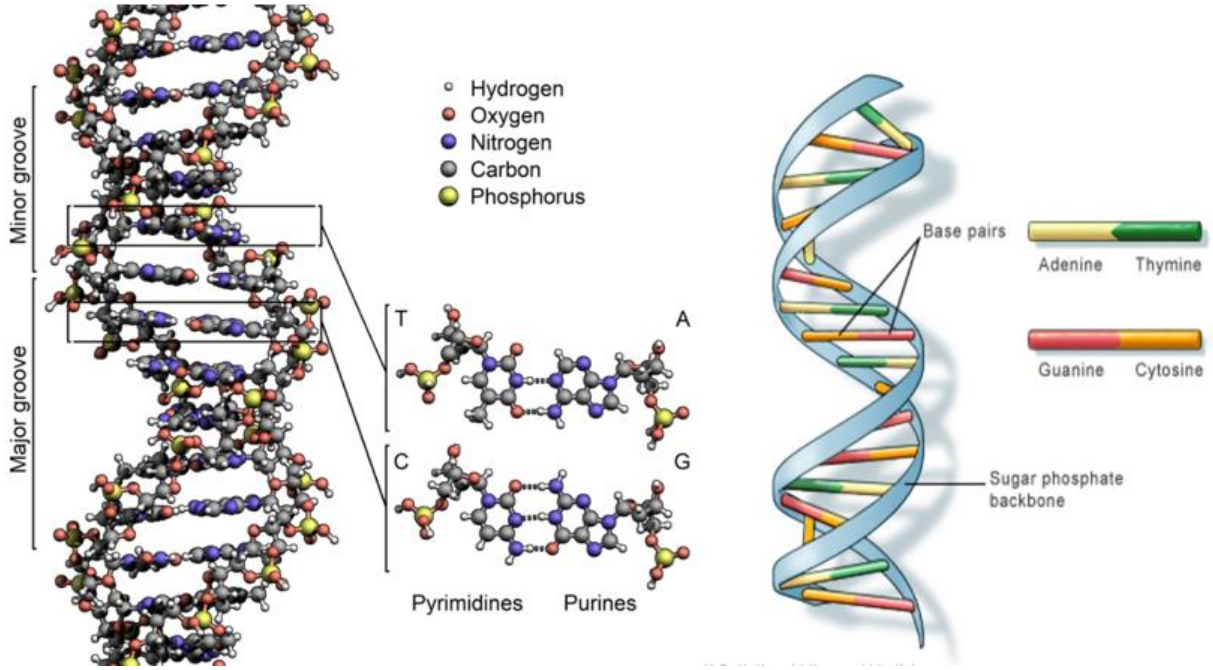

Figure 1.4: DNA structures (DNA - Wikipedia, n.d; What Is DNA?: MedlinePlus Genetics, n.d).

1.4 Dendrimers

1.4.1 Dendrimer structure

Dendrimers are considered as a type of polycations, which are organic molecules that consist of a core on the center of the molecule with branched monomer repeating units that makes it a three-dimensional structure as illustrated in Fig. (1.5), which gives it the possibility to be a polymer and soft structure. The dendrimers have generation numbers (when the branch growth goes from the core to the surface of the dendrimer) starting from G0—initial precursor, G1—first modification, G2—second modification, etc. When the generation number is increased the dendrimer becomes larger and denser. Indeed, in the lower generation, it will be soft and expected to have a more disk-like shape, but in high generations it will be hard-sphere (Janaszewska, A. et al., 2019).

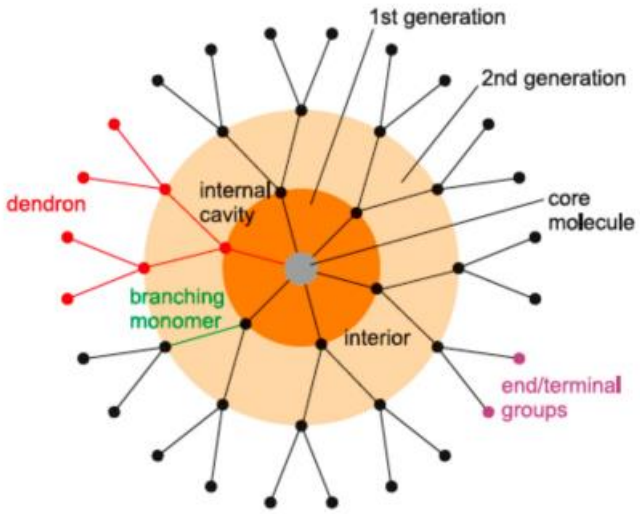

Figure 1.5: dendrimer structure (Janaszewska, A. et al., 2019).

1.4.2 Dendrimer properties

Dendrimers have many structural features, the most important are: abundant surface functional groups, various types of functionalized, precise molecular arrangements, precise nanoscale structure, highly geometric symmetry, and homologous series of cavity size. Moreover, dendrimers' compact structure and precisely calculated molecular weight (MW) are their first distinguishing features. They have characteristics of polyvalency and monodispersity. Their main characteristic is the ability to produce these nanomolecules. Additionally, the dendrimer's structure can be precisely controlled (Fatemi, S. M. et al., 2020). Modifications can be inserted at terminal end groups, and branching (topology) can be controlled. Thirdly, for therapeutic candidates, it is essential that the majority of dendrimers are soluble in aqueous solutions because this affects their high absorption and bioavailability. Finally, many dendrimers easily pass through cell membranes, improving the cellular absorption of anything complexed or conjugated with them. As a result, they exhibit a variety of performance traits, including solubility, hydrodynamic performance, distinctive viscosity behavior, and versatility (Fatemi, S. M. et al., 2020).

Table 1.1: Charge and radius of PAMAM generations as provided from the manufacturer, Dendritech. While surface charge density was calculated in this study.

Generation G	Ammonia cored dendrimer			Ethylenediamine cored		
	$\boldsymbol{Charge\ Z_d}$	$\boldsymbol{Radius\ R_s\ (nm)}$	$\boldsymbol{\sigma\ (e.nm^{-2})}$	$\boldsymbol{Charge\ Z_d}$	$\boldsymbol{Radius\ R_s\ (nm)}$	$\boldsymbol{\sigma\ (e.nm^{-2})}$
1	6	1.58	0.19	8	1.10	0.53
2	12	2.20	0.20	16	1.45	0.61
3	24	3.20	0.19	32	1.80	0.79
4	48	4.00	0.24	64	2.25	1.01
5	96	5.30	0.27	128	2.70	1.40
6	192	6.70	0.34	256	3.35	1.82
7	384	8.00	0.48	512	----	----
8	768	----	----	1024	4.85	3.46

1.4.3 Dendrimer synthesis

Fritz Vogtle, Donald Tomalia, and other researchers at George Newkome's research lab made the initial discovery of dendrimer synthesis in the late 1970s and early 1980s. The polyamidoamine (PAMAM) dendrimer which considered water soluble dendrimer, also known as Starburst polymers was one of the first dendrimers to be synthesized by Tomalia and coworkers. It is made up of repeatedly branched subunits with amide and amine characteristics.

Typically, dendrimers are synthesized using techniques that let the structure be controlled throughout every step of production. Divergent or convergent methods are primarily used to create dendritic structures (Parata et al., 2016).

1.4.3.1 Divergent method

The approach that was initially proposed and is currently the most popular is divergent growth. This approach is the result of important work by Tomalia and Newkome as well as Vögtle's branching

model research (Grayson et al., 2001). The building of the dendrimer in the divergent process begins at the core and moves outward. Two crucial steps are needed for this procedure: coupling the monomers together, and activating the end group of the monomer to facilitate the reaction with a new monomer (Boas et al., 2006). Repeating the two previous steps until the required dendrimer generation is obtained is called the divergent growth method, as shown in Fig. (1.6).

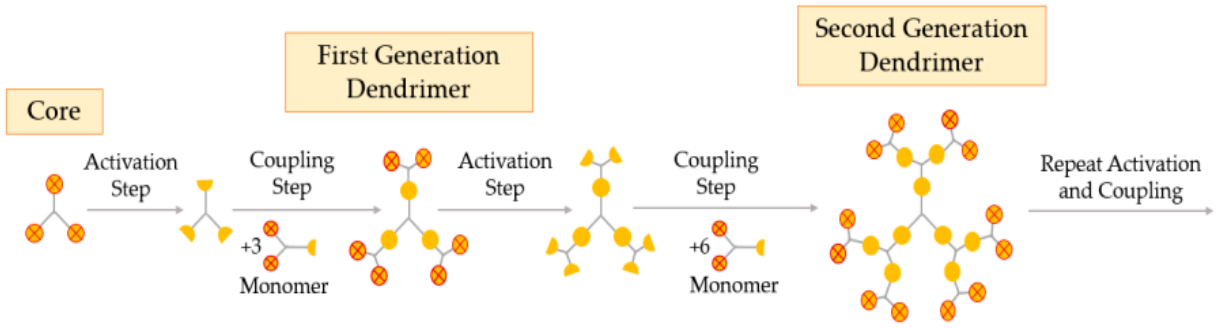

Figure 1.6: synthesis of dendrimers by the divergent growth method (Santos, A. et al., 2019).

The divergent processing begins with the core being activated or modified and the first monomer being coupled to form the first generation of the dendrimer. Next, this first generation (G1) is deprotected or activated in order to interact with other branched monomers and couple the second generation (G2), etc. A new generation is produced each time a new layer of branching units is created, where the generation number equals the number of branched layers from the core (Caminade et al., 2011). To prevent incompletely formed branches when using the divergent method, it's critical that each step of the reaction be finished before the addition of a new generation (Mendes et al., 2017). The dendrimer's surface may be quickly functionalized.

1.4.3.2 Convergent method

The convergent technique, first out by Fréchet and Hawker in 1989–1990 (Mendes et al., 2017), is an alternate approach utilized for the synthesis of dendrimers. The convergent approach creates dendrimers starting from the surface, which will finally become the outside of the structure, as opposed to the core, as in the case of the divergent process Fig. (1.6). To achieve the appropriate dendritic structure, the coupling and activation processes are repeated as part of the convergent growth approach. In order to create the dendritic segment, the surface groups, which are typically

two, are first linked to a monomer (dendron generation zero). In the second stage, this fragment is activated so that it may interact with additional monomers and form a dendron of the first generation, or a dendritic wedge. This synthetic process may be repeated to produce dendrons of a bigger generation, which can then be connected to a multifunctional core in the last stage to create the final dendrimer. At the center, where two or more dendrons are linked to form the dendrimer, the convergent synthesis's last step is completed as shown in Fig. (1.7). Steric inhibition makes it more difficult to create big dendrimers (often above the sixth generation), which lowers yields since the coupling reaction takes place at the focal point of the forming dendron (Parata et al., 2016; Grayson et al., 2001).

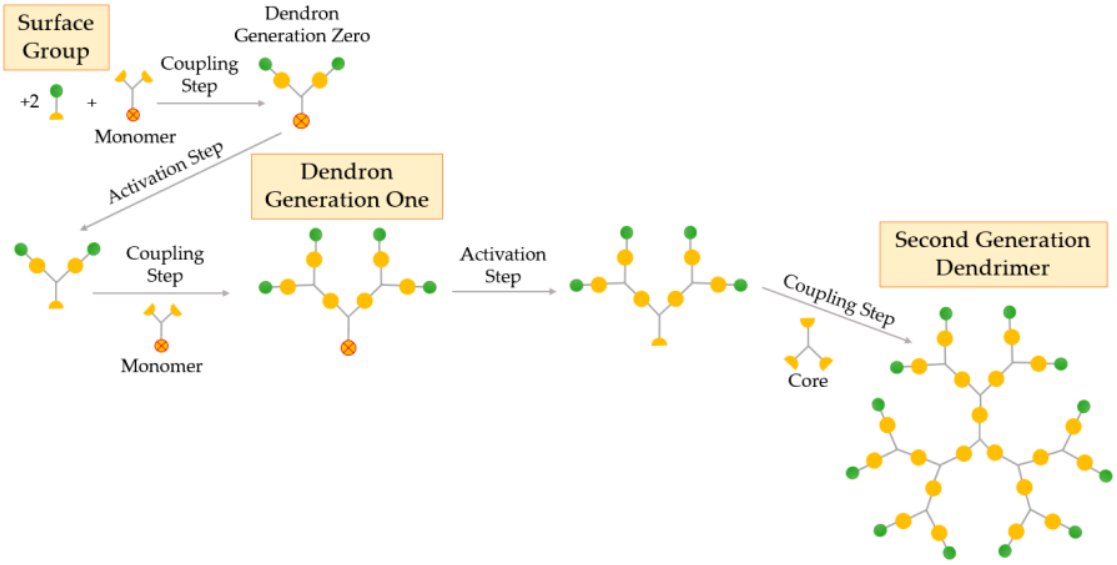

Figure 1.7: Synthesis of dendrimers by the convergent growth method (Santos, A. et al., 2019).

1.4.4 Dendrimers cytotoxicity

Dendrimer cytotoxicity is strongly influenced by the quantity and type of functional surface groups. Anionic and neutral dendrimers have minimal to no toxicity, whereas cationic dendrimers frequently show high toxicity. For instance, grafted carbosilane-poly(ethylene oxide) (CSi-PEO) dendrimers and other dendrimers terminated with neutral or anionic groups seem to be much less toxic

(Ciolkowski et al., 2012), whereas poly(amido amine) (PAMAM) and poly(propyleneimine) (PPI) dendrimers possessing terminal primary amines are characterized by concentration- and generation-dependent toxicity (Jevprasesphant et al., 2003; Malik et al., 2000). As a result, the cationic dendrimer's cytotoxicity is reduced when its surface is modified with negatively charged or neutral moieties (Malik et al., 2000). Surface functionalization with pyrrolidone, polyethylene glycol (PEG), or another biocompatible substance can drastically decrease cytotoxicity to levels that are far superior to those of currently available products (Ciolkowski et al., 2012). The interaction between negatively charged cell membranes and the positively charged dendrimer surface can be used to explain why cationic dendrimers are cytotoxic. This interaction causes the cell membrane to become damaged, causing nanopores to form, which ultimately cause the cell to die. Fig. (1.8) shows how dendrimers' bioavailability, immunogenicity, and in vitro and in vivo toxicity are influenced by their surface charge (Santos, A. et al., 2019).

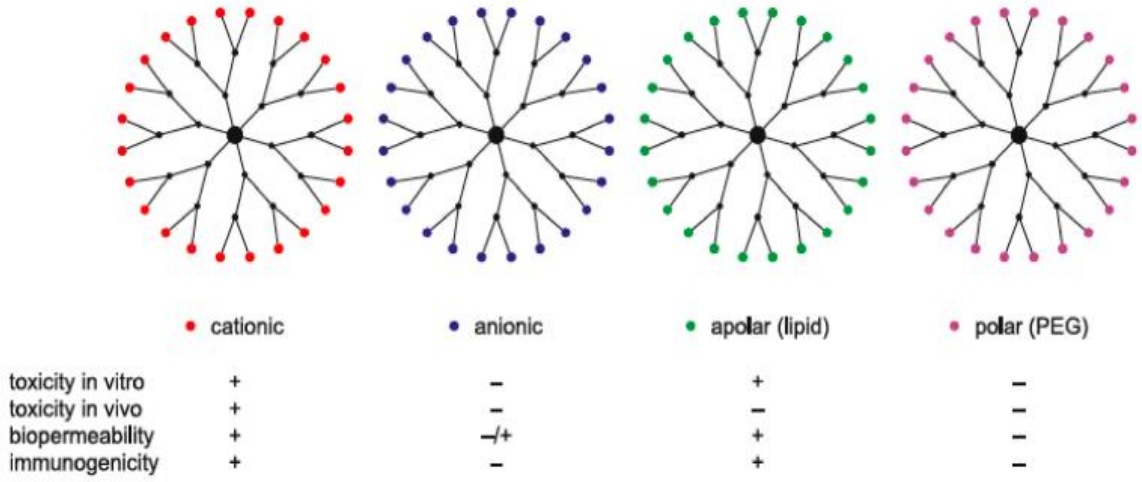

Figure 1.8: The effect of the surface charge of dendrimers on their bioavailability, immunogenicity, and in vitro and in vivo toxicity. Sign "+" indicates that there is an effect; sign "−" indicates no effect. (Santos, A. et al., 2019).

1.4.5 PAMAM dendrimers

PAMAM dendrimers are the most important type of dendrimers. They are one of the most thoroughly researched Starburst macromolecules. They are poly(amido)amine (PAMAM) dendrimers with ellipsoidal or spheroidal shapes. The PAMAM dendrimers subclass is referred to

as "Starburst dendrimers", which is considered a trademark name. The name alludes to the star-like pattern that may be seen when examining the two-dimensional structures of high-generation dendrimers of this kind. Fig. (1.9) shows the structure for generation two of PAMAM dendrimer. These polymers are typically referred to by the acronyms "PAMAM (Starburst)" or simply "Starburst." PAMAM dendrimers have diverse biomedical applications. (Facts and unresolved questions).

PAMAM dendrimers have an exterior surface made of terminal functional units and an initiator ethane-1,2-diamine core with layers of radially repeating units connected to it. The size and properties of a particular dendrimer are determined by the generation, which is made up of one of these macromolecules' branching layers. Half-generation PAMAM dendrimers finish with carboxylic acid groups, whereas full-generation dendrimers conclude with amine groups. Fig. (1.10) shows dendrimer terminal groups. Thus, depending on their termini, interior functions, and pH, a dendrimer host's interior and/or exterior can be cationic, anionic, or non-ionic (Labieniec, M. et al., 2009).

These dendrimers have primary amine functional groups at every branch end. The diameter of PAMAM dendrimers ranges from 1 nm to 14 nm. These dendrimers have great potential as gene carriers. Therefore, it can be a good candidate to condense DNA. This type of dendrimer is widely studied and commercially available. It consists of ethylene diamine core and amide repeating units. This dendrimer has been found in biomedical applications and composite base materials (Fatemi, S. M. et al., 2020).

1.4.6 Application of PAMAM in DNA

PAMAM dendrimers have various applications, especially as a carrier of DNA. Therefore, it’s important to study the bonding between DNA and PAMAM dendrimers. However, by using MD simulations and calculating free energy, the study of sequence-dependent complexation between single-strand DNA (ssDNA) and various generations of EDA-cored PAMAM dendrimers was done by Maiti and Bagchi (PAMAM dendrimer based macromolecules and their potential applications: recent advances in theoretical studies). They found that in solution, ssDNA is far from PAMAM for

generations 2 and 3. Hence, ssDNA could not be neutralized due to a lack of surface charge for these two generations. On the other hand, another study by Nandy and Maiti et al. (Nandy B et al., 2010), investigated the complexation between generations 3 to 5 and dsDNA. They demonstrated that DNA can be completely wrapped around PAMAM-G5 dendrimers. This reveals the pivotal effect of dendrimer positive charge and the genetic material negative charge on the conformation structure of the complex.

Many of the distinctive characteristics of dendrimers, including their particular solubility and reactivity, are due to the chemical makeup of the outer functional groups. Due to their high reactivity, functional surface groups allow dendrimers to be modified or conjugated with a wide range of intriguing guest molecules. Thus, PAMAM dendrimers' highly branched, multivalent, and multifunctional surfaces enable modification of their surface chemistry, and their internal core's relative solvent content makes them beneficial for a variety of medicinal applications across a wide range of sectors. Among these applications are the encapsulation and solubilization of pharmaceuticals, the transport of DNA or oligonucleotides, or the creation of targeted delivery systems employing dendrimers as carriers for pharmaceutical administration via the gastrointestinal tract (Labieniec, M. et al., 2009).

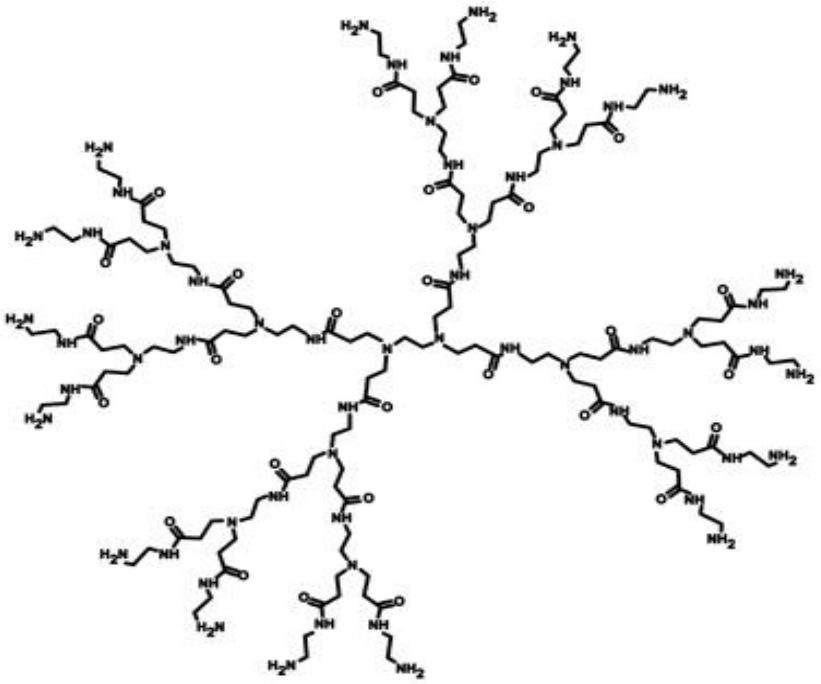

Figure 1.9: Generation 2 PAMAM Dendrimer (for larger view), (PAMAM Dendrimers, 2018).

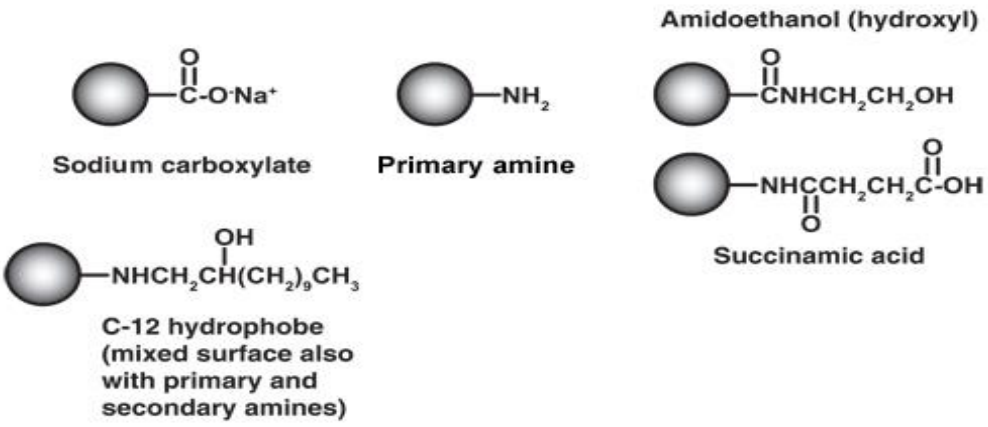

Figure 1.10: Dendrimer Terminal Groups (for larger view), (PAMAM Dendrimers, 2018).

1.5 Modified dendrimers

DNA wrapping around the dendrimer forms a complex conformation that allows the DNA to access its target site, but it was found that dendrimers have highly charged surfaces leading to cell injury and damage as they can generate pores on the cell membrane. In previous studies, they found that dendrimer implantation might disrupt the bilayer's structure and influence the fluidity of the membrane. Smith et al. (Smith et al., 2010) discovered via solid state NMR that G5 and G7 dendrimers reduced the acyl chains' flexibility in 1,2-Dimyristoyl-sn-glycero-3-phosphocholine supported lipid bilayers (DMPC SLBs). It was believed that partial incorporation of PAMAM dendrimers would create a void zone in the membrane, which would increase the mobility of the acyl chains and thin the bilayer. Mecke et al. (Mecke et al., 2005) studied the interactions between the MSI78 polymer, an analog of an antimicrobial observed in frog's skin, and a DMPC SLB using AFM and NMR, and they also observed this result (Fox, L. J. et al., 2018).

Thus, to reduce surface charge density by adjusting the media of complexation using some methods such as acetylation, succination, and PEGylation. Examples of modified PAMAM dendrimers illustrated in Table (1.2). Acetylation is a reaction to neutralize the positive surface charge of the particles by the addition of an acetyl group to a compound as illustrated in Fig. (1.11).

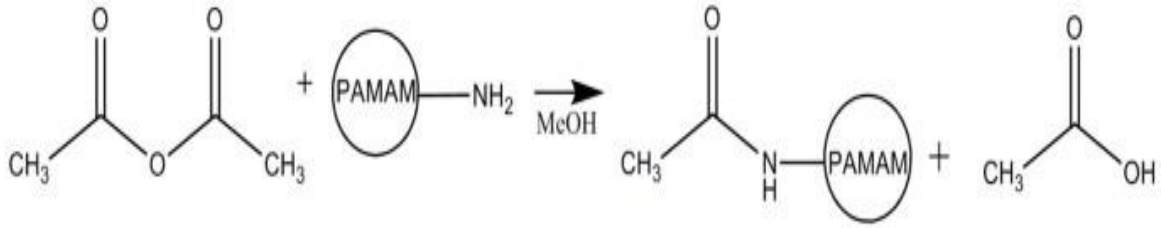

Figure 1.11: Acetylation of PAMAM dendrimers. Acetic anhydride reacts with primary amines of G5 PAMAM dendrimers to produce acetylated PAMAM (Waite et al., 2009).

Table 1.2: Illustrates modified PAMAM dendrimers with different generations, molecular weights and end groups (PAMAM Dendrimers, 2018).

Generation	Molecular Weight*	End Groups*
HYDROXY SURFACE PAMAM		
PAMAM Dendrimer G2-OH	3272	16
PAMAM Dendrimer G3-OH	6941	32
PAMAM Dendrimer G4-OH	14279	64
PAMAM Dendrimer G5-OH	28954	128
PAMAM Dendrimer G6-OH	58304	256
PAMAM Dendrimer G7-OH	117005	512
SUCCINAMIC ACID SURFACE PAMAM		
PAMAM Dendrimer G2-SA Succinamic acid	4856	16
PAMAM Dendrimer G3-SA Succinamic acid	10109	32
PAMAM Dendrimer G4-SA Succinamic acid	20615	64
PAMAM Dendrimer G5-SA Succinamic acid	41626	128
PAMAM Dendrimer G6-SA Succinamic acid	83648	256
SODIUM CARBOXYLATE SURFACE PAMAM		

PAMAM Dendrimer G0.5 Caboxylate Sodium Salt	1269	8
PAMAM Dendrimer G1.5 Caboxylate Sodium Salt	2935	16
PAMAM Dendrimer G2.5 Caboxylate Sodium Salt	6267	32
PAMAM Dendrimer G3.5 Caboxylate Sodium Salt	12931	64
PAMAM Dendrimer G4.5 Caboxylate Sodium Salt	26258	128
PAMAM Dendrimer G5.5 Caboxylate Sodium Salt	52913	256
PAMAM Dendrimer G6.5 Caboxylate Sodium Salt	106222	512
PAMAM Dendrimer G7.5 Caboxylate Sodium Salt	212841	1024
HYDROPHOBE SUBSTITUTED PAMAM		
PAMAM Dendrimer G2-25% C12 Hydrophobe	4730	Mixed amine/hydrophobe
PAMAM Dendrimer G2-50% C12 Hydrophobe	6205	Mixed amine/hydrophobe
PAMAM Dendrimer G3-25% C12 Hydrophobe	9857	Mixed amine/hydrophobe
PAMAM Dendrimer G3-50% C12 Hydrophobe	12807	Mixed amine/hydrophobe

PAMAM Dendrimer G4-25% C12 Hydrophobe	20112	Mixed amine/hydrophobe
PAMAM Dendrimer G4-50% C12 Hydrophobe	26010	Mixed amine/hydrophobe

1.5.1 Effect of acetylation

To precisely functionalize the principal surface amines, the reactive end groups of G5 poly(amidoamine) (PAMAM) dendrimers have been acetylated. These dendrimers are more water-soluble when they are acetylated, which is essential for biological applications that call for solubility in aqueous solutions. One can create soluble polymers that operate as a scaffold for further functionalization by controlling the precise proportion of acetylated end groups and the dendrimer structure (Majoros, I. J. et al., 2003).

Hwankyu and Ronald (Hwankyu Lee and Ronald G. Larson, 2006) studied the effect of 0%, 50% and 100% acetylation for G3 and G5 dendrimers on their radii of gyration using coarse-grained model. They confirmed that the radii of gyration were computed, and the results demonstrate that the Rg values for dendrimers significantly decrease with time once the simulations start. Moreover, when compared to unacetylated dendrimers, the more acetylated G5 dendrimers exhibit lower Rg values (Lee, H. et al., 2006).

Hwankyu Lee et al. performed molecular dynamics simulations of 0% and 90% acetylated G5 PAMAM dendrimers in explicit water and methanol. These dendrimers are labeled "G5", "G5M," "G5-Ac90," and "G5M-Ac90" in this instance. Fig. (1.12) demonstrate snapshots of the simulations that show that all dendrimers shrink and form ellipsoidal spheroids in their final conformations, with G5Ac90 and G5MAc90 becoming more compact than G5 and G5M. Also, they demonstrated that at the start of the simulations, the Rg values for G5, G5M, G5-Ac90, and G5M-Ac90 dramatically decreased as functions of time (Lee, H. et al., 2006).

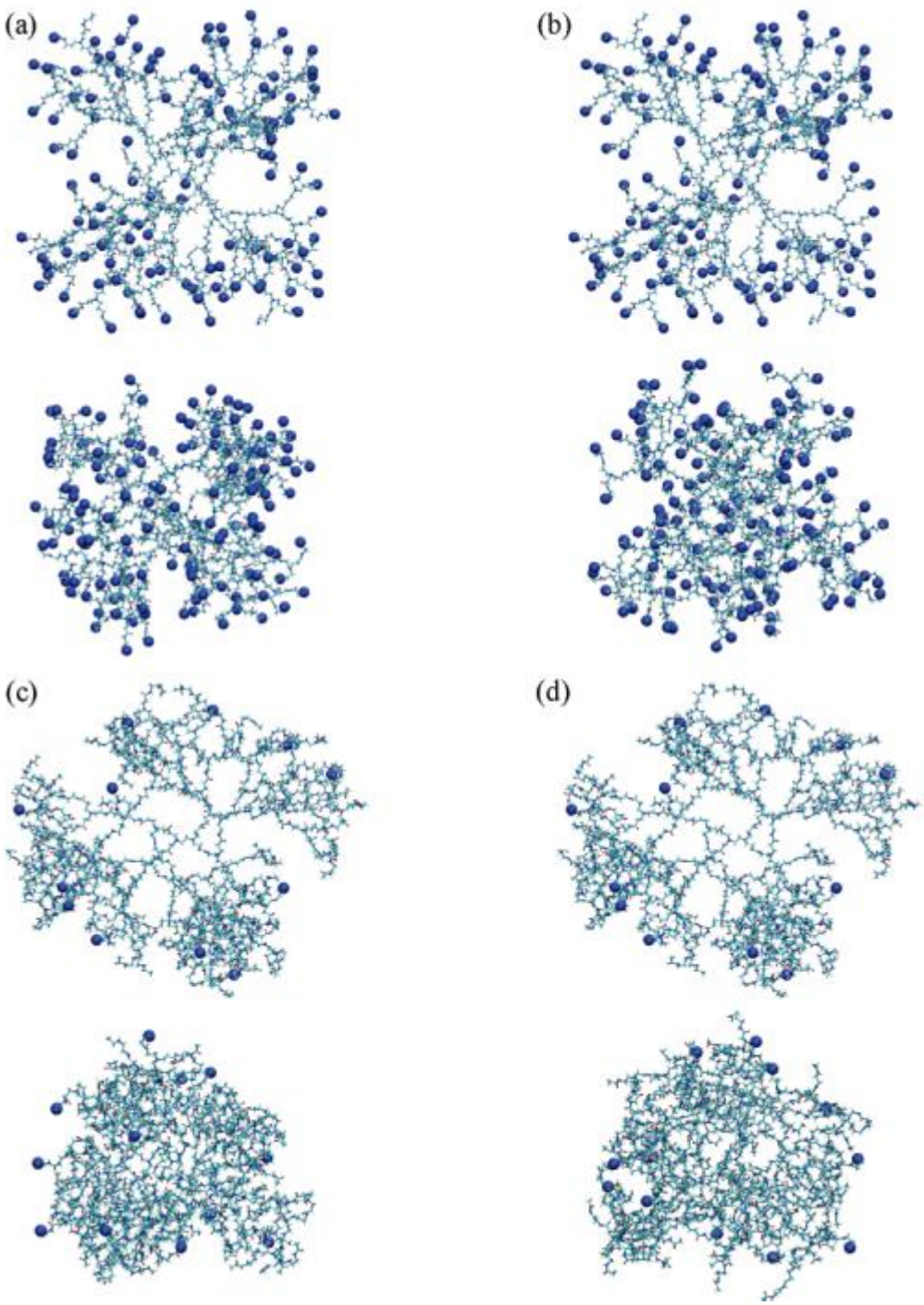

Figure 1.12: Snapshots at the beginning (0 ns, top images) and end (4.9 ns for G5, 4.5 ns for G5M, 6.4 ns for G5-Ac90, and 5.0 ns for G5M-Ac90, bottom images) of (a) G5, (b) G5M, (c) G5-Ac90, and (d) G5M-Ac90 simulations. Protonated surface residues (NH3 +) are shown as blue dots. The explicit water molecules and counterions are omitted for clarity (Humphrey, W. et al., 1996).

1.6 Charge Inversion (overcharging)

Neutralizing DNA with dendrimer or with other types of positively charged particles will reduce the negative charge of DNA. Thus, reducing the repulsion force between the DNA and the cell membrane which facilitates and allows the DNA to condense the positively charged particle and to penetrate the cell membrane without damaging or disrupting it. This phenomenon is called charge inversion as illustrated in Fig. (1.13), means the charge of the DNA is inverted from negative charge to positive one. We can find this phenomenon in-vivo; for example, when a negatively charged DNA wraps around a positively charged histone octamer to form a complex called a nucleosome.

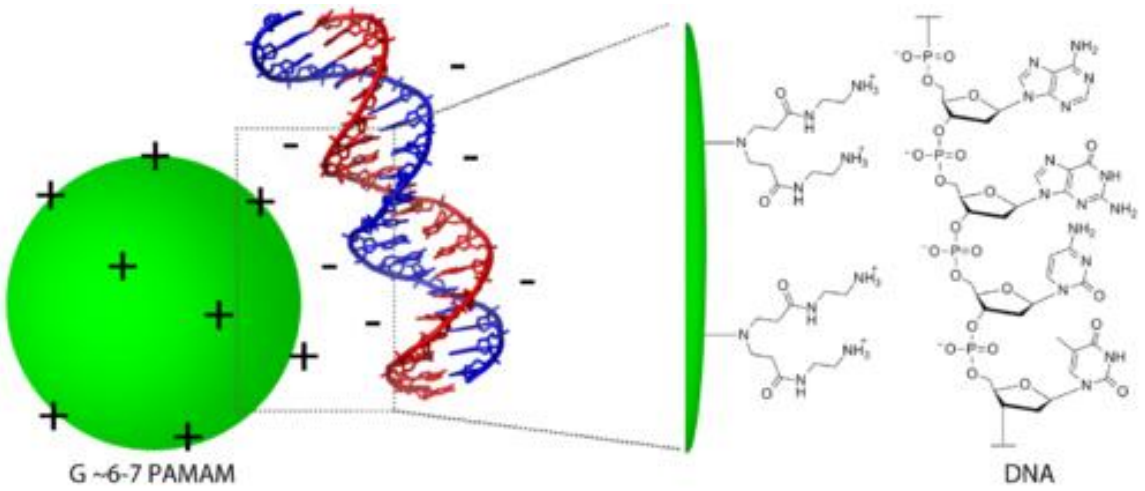

Figure 1.13: Negatively charged DNA with positively charged PAMAM dendrimer.

1.7 Polyelectrolyte/dendrimer complexation.

Gene materials and dendrimers may form complexes with linear polyelectrolytes (PEs), such as RNA or DNA, based on electrostatic interactions that are useful for delivery. For instance, experiments for determining and validating new drug targets as well as for studying gene function have reported the delivery of short interfering RNAs (dsRNAs) into target cells using PAMAM dendrimers (Liu, X. et al., 2012). The stiffness of linear gene materials varies. The experimental values of DNA's single-stranded DNA (ssDNA) and double-stranded DNA (dsDNA) persistence lengths l_p range from 0.75 to 3.0 nm and 50 nm, respectively. for RNA there is a wide variety of l_p.

These experiments have been demonstrated that the stiffness of the linear PEs affects the structures of the complexes (Chen, H., et al., 2012; Merkel, O. M., et al., 2010).

Recently, Maiti and coworkers (Maiti, P. K. et al., 2006) used atomistic molecular dynamics simulations to study dendrimer-ssDNA complexes. They showed that when the dendrimer has sufficient positive charges to neutralize the charges on the ssDNA, the ssDNA can wrap around the dendrimer and significantly penetrate into it. Additionally, they noted that due to a competition between the ssDNA's binding enthalpy and bending rigidity, the stability of the complexes is extremely sensitive to the sequence of the ssDNA.

Lyulin and coworkers (Lyulin et al., 2008) carried out extensive coarse-grained molecular dynamics simulations on the complexes made up of a fourth generation cation dendrimer, a relatively short anionic chain with explicit counterions, and solvent molecules. They concentrated on understanding the impact of counterions and PE chains with different valences, also explain the strength of electrostatic interactions and how it affected the properties of complexes. Therefore, the creation of a stable complex during equilibration was achieved by the electrostatic interactions, and this is true for all Bjerrum length values that were taken into consideration.

1.8 Effect of salt on complexation.

Addition of salt also changes and affects the complexation in different manners. For instance, the effect of salt concentration was studied for G3-G6 PAMAM dendrimer from 10-1000 mM (Yu, S. 2013), based on the radius of gyration Rg values from the work of Maiti et al. (Maiti et al., 2005) The results revealed that when the salt concentration increases, the radius of gyration decreases.

Boroudjerdi et al (Boroudjerdi, H., et al., 2011), also studied the effect of salt concentration on the structural features of the complex fiber. The salt concentration used ranged from 0 up to 100mM of monovalent salt with the invers screening length K ranging from 0 to 1.1 nm-1. For macroion charge Z = 15, and for chain length per unit cell L = 68 nm. As a result, by altering the salt concentration, the findings reveal many of the helical fibers that can be seen in Fig. (1.14) and indicate significant structural changes. However, as can be observed, chain complexation increases as salt

concentrations increase. At intermediate salt concentration, the strongly wrapped states appear, and are induced by electrostatic chain-sphere attraction, which overcomes the chain (electrostatic and bending) self-energy.

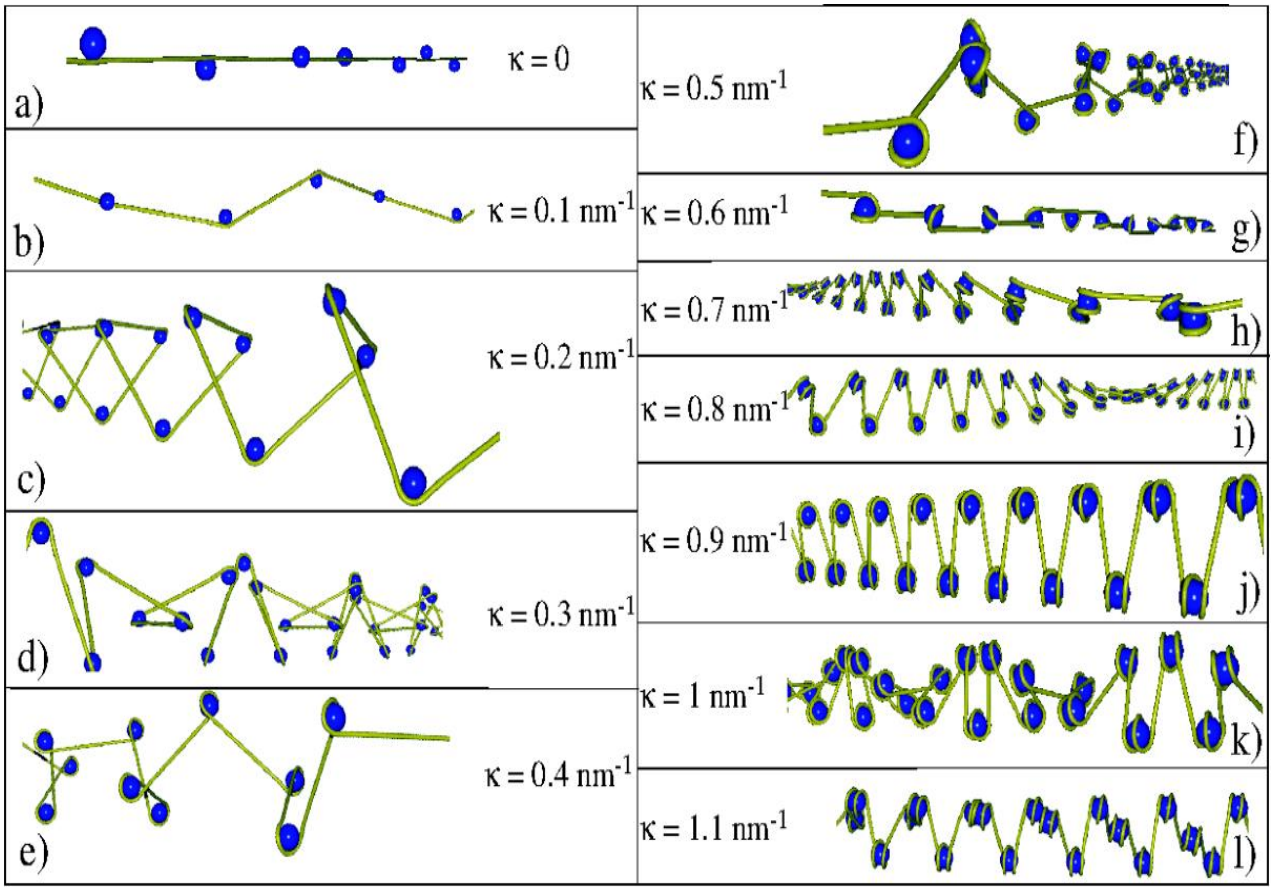

Figure 1.14: The optimal spatial configuration of the complex fiber, for macroion (sphere) charge valency Z = 15, total chain length per unit cell (per sphere) of chain length = 68 nm (equivalent to 200 DNA base pairs) and for various Debye inverse screening lengths as indicated on the graph. (Boroudjerdi, H., et al., 2011).

1.9 Literature Survey

Netz, et. al (1999), studied theoretically the complexation between a positive charge sphere with an opposite charged semiflexible polyelectrolyte (charged polymer) depending on two parameters; salt concentration and a bare stiffness of the polymer. Also, they used perturbational scheme to calculate the classical or optimal path of the polymer and to determine its structure. As a result, a strong compaction and full wrapping of polyelectrolyte around the sphere happens at high sphere charge and at an intermediate salt concentration. At low salt concentration, the polymer partially wraps around the sphere. While at high salt concentration, the polymer arms extend in an un-ordered way from the sphere in which the wrapping of the polymer was also partial.

Maiti, et. al (2006), used atomistic molecular dynamics simulations based on some free energy calculations to study the complexation between DNA and PAMAM dendrimer with different generations to show if it is sequence dependant or not. Also, these simulations were followed by inherent structure determination. As a results, they verified and confirmed a strong sequence dependence and stable complexation. In addition, they found that the free energy surface ruggedness was increased due to wrong base pairing along the condensation track.

Rohit B. Kolhatkar et. al (2007), investigated the cellular uptake on Caco-2 cell monolayers. Also, they studied the effect of the acetyl group on cytotoxicity by modifying the surface groups of amine-terminated PAMAM dendrimers G2 and G4 with acetyl groups. As a result, modification by acetylation reduced the cellular toxicity while preserving permeability through the cell monolayer.

Waite, et. al (2009), studied the RNA/dendrimer complex interactions focusing on the effect of acetylation PAMAM dendrimer generation 5, which reveals how this affect the delivery of siRNA to the cell. As a result, the cytotoxicity of the dendrimer is reduced to U87 by increasing amine acetylation.

Chen, et. al (2011), studied and characterized the DNA/polyamidoamine G4 dendrimer by different degrees of DNA bending, using synchrotron SAXS and a scattering function calculation of model structures to show three distinct nanostructures. In this research they studied the charge density dendrimer. As a result, they confirmed that the DNA penetrated around the dendrimer with high

charge density while wrapping. Thus, the structure transformed from a square columnar mesophase to hexagonally-packed superhelices.

J.S.Klos (2011), employed monte Carlo simulation and used the bond fluctuation method to study and investigate oppositely charged polyelectrolytes of various lengths and G4 dendrimer with Nt charged terminal groups accompanied by neutralizing counterions in an a thermal solvent. Their results show us that at intermediate temperature the electrostatic effects cause swelling for dendrimers. While at the two lowest temperatures the overcharging phenomenon is considered for chains longer than the compensation point. Therefore, the effect of temperature was also observed on the distribution of tail lengths of the adsorbed chain, which also depends on the length of the chain. At higher temperatures, random fluctuation of tail lengths takes place, and a long and short tail is formed at intermediated temperatures. Finally at the lowest temperatures, two tails of equal lengths are preferred.

Qamhieh, et. al (2013), studied the formation and interactions of DNA, which is considered a semiflexible polyelectrolyte, and oppositely charged dendrimers with different generations. They assumed that the sphere is a soft sphere by applying the theoretical model and by using experimental data from previous studies. In this study, they focused on some parameters such as zeta potential which determines if the DNA/dendrimer system will be stable or will coagulate depending on the electrostatic attractions, dielectric constant, and inverse debye length. Also, they focused on the charge ratio between the phosphate groups on the DNA and the charged groups on the dendrimer surface. As a result, they found that as the dendrimer generation increases, the number of DNA wrappings around the dendrimer will increase. For higher generation dendrimers, they found that the net charge of segment DNA/dendrimer complex is negative. While for the lower dendrimer generations, the net charge was positive which means the possibility for the dendrimer to change from its original to the contracted state.

Boroudjerdi, et. al (2014), studied the conformation of the polyelectrolyte chain/nanosphere strongly coupled complex by employing the primitive chain sphere model, therefore investigating the global phase behavior. In this study, they neglected the thermal fluctuation, the excluded volume interaction between chain segments, and the twist degree explicitly in certain polyelectrolyte was also neglected. While, the energetic ground state was dominant. They investigated the

conformational changes by changing the control parameters; including the contour length, linear charge density, and persistence length. To do that they utilized a rescaled representation to obtain results that can be applied to a broad range of polyelectrolyte/nanosphere complexes. As a result, they determined the chain conformation wrapping around the sphere by the competition between two interactions; one of them tend to wrap the chain around the sphere which is the electrostatic attraction between them. While the others allow to unwrap the chain from the sphere. These interactions are the chain elasticity and the electrostatic repulsion between chain segments.

Qamhieh, et. al (2014), studied a theoretical model that presented a polyelectrolyte wrapping around a dendrimer with different generations by using different factors and parameters such as Bjerum length, salt concentration, dendrimer charge, and persistence length of the polyelectrolyte to show their effect on complexation of dendrimers with LPE. As a result, they developed and verified the optimal wrapping length of the chain adsorbed on the dendrimer.

Shi, et. al (2016), studied nanoparticles aggregation by focusing on different parameters that controls fractal dimension Df of a nanoparticle with a positively charged nanoparticle such as; persistence length, ionic strength, salt concentration, and the main parameter the total persistence length divided by the nanoparticle size Lt/R. The conformation was investigated by using small-angle neutron scattering. As a result, the fractal dimension Df was tuned. In addition, at high ionic strength larger fractal dimension was observed. Moreover, Lt/R has had the main effect on nanoparticle conformation; Df = 1 For Lt/R ≥ 1 low ionic strength was found. On the other hand, for Lt/R < 1 in excess of nanoparticles, an increase in Df up to 2 was found.

Daniel L.Z Caetano and et al (2020), studied the properties of multichain adsorption of polyelectrolytes as a flexible charged chains onto oppositely charged spherical nanoparticles (SNPs) by using monte Carlo simulation. They studied the degree of fluctuations of the PE-SNPs electrostatic energy. To describe this phenomenon, they applied the linear and nonlinear Poisson-Boltzmann theories. Also, they focused on the effect of the SNPs charge density and the salt concentration on the critical adsorption- the phase separation curve between the adsorbed and desorbed state of polyelectrolytes. And they tried to extend this research for critical adsorption of a single polyelectrolyte onto SNP. As a result, the linear Poisson-Boltzmann theory was inapplicable and the nonlinear theory was the topic of this research. In addition, they found exact parameters for

all the subtransitions which emergence splitting of the critical adsorption boundaries for adsorbed and desorbed polyelectrolytes at low-salt conditions. These results can extend for critical adsorption of a single polyelectrolyte onto the SNP.

Gupta, et. al (2020), studied the conformational properties of polyelectrolyte/ poly (propylene imine) dendrimers complexes at neutral pH in an aqueous solution by using molecular dynamics simulations. They confirmed that a conformational transition of the polyelectrolyte wrapping around the dendrimer changed from a dense form to an extended form with an increase in the PE chain length. They found that the charge distribution of the polyelectrolyte/ poly (propylene imine) dendrimers complexes showed that the lower generation of dendrimers is overcompensated by the longer polyelectrolyte chain in the complexes leading to an overall negative charge. On the other hand, for higher generation dendrimers there is no neutralization of the charge found by the polyelectrolyte chain in the complexes which introduce an overall positive charge of the polyelectrolyte/ poly (propylene imine) complexes. The results were confirmed by an increased cavity volume in these complexes with an increase in polyelectrolyte chain.

Shilpa Gupta et.al (2020), applied molecular dynamic simulation to study the conformational properties of polypropylene imine PPI dendrimer – PE complexes with oppositely charged linear polyelectrolyte chains at neutral pH. They investigated some conformational properties, such as the atomic density profile, cavity volume, counterion density distribution, charge distribution, and the static structure factor (as a function of the charge and chain length of the LPE). As a result, a conformational transition of the dendrimer–PE complexes (as a function of the PE chain length) from compact to an open structure corresponds with a longer PE chain. At the same time, an increase in the cavity volume in dendrimers was noticed. On the other hand, a dense structure was observed when a short PE chain was encapsulating within the dendrimer.

Sehui Bae et.al (2021), applied molecular dynamic simulations to investigate the effect of DNA flexibility on the complex formation of a cationic nanoparticle NP and a DNA fragment using the Martini DNA model. Therefore, the structure of a complex formed between a cationic NP and a DNA fragment was determined by DNA flexibility using various persistence lengths. As a result, when the electric charge of a cationic NP increases the degree of DNA bending increases. Thus, the

more flexible DNA fragment bends and wraps around the NP. On the other hand, the less flexible DNA fragment wraps around the NP without significant wrapping.

Khawla Qamhieh et.al (2022), studied the complexation between PAMAM dendrimers with DNA in which she investigated the linker between these complexes in some environments, such as pH and bjerum length by using a penetrable sphere model. As a result, the complexation between dendrimer and DNA was tuned. Moreover, when the pH increased the linker was increased and decreased when bjerum length is increased.

1.10 Statement of the problem and the Objectives

The compaction of acetylated dendrimers with a single DNA and other polyelectrolytes is studied. Acetylation of the dendrimer will change the surface charge and the size of the dendrimer, which will affect on the complexation and how much of the DNA will be wrapped around the dendrimer. Through our study we compared between the wrapping length of the polyelectrolyte around the normal dendrimers and around the acetylated ones.

Chapter Two

Model And Methods

2.1 Introduction

Based on the theoretical model that was developed by Qamhieh et al (Qamhieh et al., 2014), we made some changes for the type of the sphere. We built our model by using soft sphere rather than hard sphere. The soft sphere is considered as a dendrimer of a radius R, and total charged Ze, where e is the elementary charged. The oppositely charged polyelectrolyte chain which considered as DNA having persistence length l_p, contour length L, and radius r = 1 nm. This polyelectrolyte also has a charge density = -e/b, which denote the elementary charge divided by the space between the charges. The experimental system is in a monovalent electrolyte (salt concentrations) that screens the charges on the soft(penetrable) sphere and the polyelectrolyte by employing an inverse Debye screening length K^{-1} = (8лCsl_B) −1/2 where $l_B = {e^2}/{\varepsilon K_B T}$ is the Bjerrum length which is equal 0.7, and $K_B T$ is the thermal energy. The K^{-1}= 3 nm due to performing the experiment in 10 mM NaBr aqueous solutions. In water (with the dielectric constant ε) and at room temperature (T=300 K)

2.2 Complexation of a LPE chain with a single sphere

We shall apply some expressions that induce several dimensionless parameters which will affect the wrapping of the polyelectrolyte on a sphere and affect the structure of a complex. The dimensionless for the total free energy of a single polyelectrolyte wrapping around hard sphere can be written as:

$$U = U_{compl(l)} + U_{chain(L-l)} + U_{compl-chain(l)} + U_{elastic(l)} \qquad (1)$$

The first term of in this equation represents the electrostatic charging free energy of a spherical complex of charge eZ(l), the second term represents the total entropic electrostatic free energy of the remaining chain ($L - l$), the third term represents the electrostatic free energy of the interaction between the complex and the remaining of the chain, and the fourth one represents the elastic (bending) free energy. Some changes and modification have been done on the first and third terms as revealed in Eq. 7 and Eq. (8-12) respectively.

Where l denotes the length of the part of polyelectrolyte (DNA molecule) condensed on the dendrimer, and the remaining chain denoted by the symbol ($L - l$).

The second term can be written as:

$$U_{chain(L-l)} \cong \frac{KT}{b}\Omega(r)(1-\xi^{-1})(L-l) \qquad (2)$$

Ω(r) represents the condensed DNA counterions which equal $2\ln(4\xi k^{-1})/r$**,** and $\xi = l_B/b$ denotes Manning parameter.

And fourth term can be written as:

$$U_{elastic(l)} \cong \frac{KT}{b}\Omega l \qquad (3)$$

Based on Ohshima et al (Ohshima et al., 1993), by using the electrostatic charging free energy of weakly charged ion-penetrable sphere of charge Ze, the first and third terms can be derived and can be written as:

$$\varphi_{sphere} = \frac{\rho}{\varepsilon}\,\frac{\exp(-kR)}{k^2}\left[\cosh(kR) - \frac{\sinh(kR)}{kR}\right] \qquad (4)$$

replace for $\rho = (Q/\frac{4}{3}\pi R^3)$,

which describes the uniform volume charge density of the sphere, and can be written as:

$$\varphi_{sphere} = \frac{3Q}{4\pi\varepsilon(kR)^2}\frac{exp(-kR)}{R}\left[\cosh(kR) - \frac{\sinh(kR)}{kR}\right] \qquad (5)$$

Where Q denote the charges distributed around the sphere (the total charge).

Integrating Equation (5) to give:

$$U_{shpere} = \int_0^Q \varphi dQ = \frac{3Q^2}{8\pi\varepsilon(xR)^2}\frac{exp(-xR)}{R}\left[\cosh(xR) - \frac{\sinh(xR)}{xR}\right] \qquad (6)$$

And replace for Q by eZ(l)

$$U_{compl(l)} = \frac{3}{8\pi}\frac{Z^2(l)KT}{(kR)^2}\frac{exp(kR)l_B}{R}\left[\cosh(kR) - \frac{\sinh(kR)}{kR}\right] \quad (7)$$

By employing a similar equation to the Debye-Huckel interaction energy of the chain end with the sphere (Netz et al., 1999). The third term in Equation (1), can be derived as:

$$dU_{compl-chain} \cong \varphi_{compl}(r) \times dq_{chain} \quad (8)$$

Where $dq_{chain} = \lambda_{chain} \times dr$

Replace for $dq_{chain}\ and\ \varphi_{compl}(r)$ in Equation (8)

$$dU_{compl-chain} \cong \frac{3Z(l)e}{4\pi\varepsilon(kR)^2}\frac{\exp(-kR)}{r}\left[\cosh(kR) - \frac{\sinh(kR)}{kR}\right]\frac{edr}{b} \quad (9)$$

$$\frac{U_{compl-chain}}{KT} \cong \frac{3Z(l)l_B}{4\pi x(xR)^2}\left[\cosh(xR) - \frac{\sinh(xR)}{xR}\right]\int_R^{L-l}\frac{\exp(-xr)}{r}\frac{dr}{b} \quad (10)$$

Substitute x by k :

$$\frac{U_{compl-chain}}{KT} \cong \frac{3Z(l)l_B}{4\pi x(kR)^2}\left[\cosh(kR) - \frac{\sinh(kR)}{kR}\right]\int_R^{L-l}\frac{\exp(-kr)}{r}\frac{dr}{b} \quad (11)$$

Where $l_B = \frac{e^2}{\varepsilon KT}$

$$F_{compl-chain}(l) \cong \frac{3Z(l)l_B k_B T}{4\pi(kR)^2}\left[\cosh(kR) - \frac{\sinh(kR)}{kR}\right] \times \left[\ln(r) - \sum_{n=0}^{\infty}\frac{(-1)^n}{(n+1)!.\,(n+1)}\right]\Bigg|_{R}^{L-1} \quad (12)$$

2.3 Calculation of the free energy for the dendrimer/DNA aggregate

When we have more than one penetrable sphere (considered as dendrimer) and one polyelectrolyte, the total free energy can be written as:

$$U(N,l) = \left\{N\left[U_{compl(l)} + U_{compl-chain}(L-Nl) + U_{elastic}(l)\right] + U_{chain}(L-Nl) + U_{int}(N,l)\right\} \quad (13)$$

Where:

N is the number of penetrable sphere, $U_{compl-chain}(L-Nl)$ denotes the electrostatic interaction between one complex and the remaining chain of length $(L-Nl)$, $U_{chain}(L-Nl)$ denotes the total entropic free energy of the remaining chain of length (L − Nl), and $U_{int}(N,l)$ denotes the interaction between the spheres.

To describe $U_{compl-chain}(L-Nl)$ from equation (13) we shall change the limit of integration to be from R to $(L-Nl)$, based on equation (10), to derive a new equation:

$$\frac{U_{compl-chain}(L-Nl)}{KT} \cong \frac{3Z(l)l_B}{4\pi(xR)^2}\left[\cosh(xR) - \frac{\sinh(xR)}{xR}\right] \times \int_{R}^{L-Nl}\frac{\exp(-xr)}{r}\frac{dr}{b} \quad (14)$$

We can give more description for $U_{chain}(L-Nl)$ by written it as:

$$U_{chain}(L-Nl) \cong \frac{KT}{b}\Omega(a)(1-\xi^{-1})(L-Nl) \qquad (15)$$

The electrostatic repulsion between all complexes and within one chain gives us $U_{int}(N,l)$ which this term can affects the structure of the polyelectrolyte chain.

Based on Ohshima et al (Ohshima et al., 1993), the free energy interaction between two penetrable spheres is written by:

$$U_{sphere-sphere} = \frac{4\pi R^2\rho^2}{\varepsilon k^4}\frac{\exp\left(kD(N,l)\right)}{D(N,l)}\left[\cosh(kR) - \frac{\sinh(kR)}{D(N,l)}\right]^2 \qquad (16)$$

where $D(N.l) = (1-NL+2NR)/N$ represents the distance between two spheres standing near to each other from the core-to-core of each one, which these two spheres should have equal wrapping lengths. Replace for the volume charge density:

$$U_{sphere-sphere} = \frac{9Q^2}{4\pi\varepsilon(kR)^4}\frac{\exp\left(kD(N,l)\right)}{D(N,l)}\left[\cosh(kR) - \frac{\sinh(kR)}{kR}\right]^2 \qquad (17)$$

Replace for Q by eZ(l)

$$U_{compl-compl} = \frac{9Z^2(l)KTl_B}{4\pi(kR)^4}\frac{\exp\left(kD(N,l)\right)}{D(N,l)}\left[\cosh(kR) - \frac{\sinh(kR)}{kR}\right]^2 \qquad (18)$$

The total interaction free energy between N spheres expressed as:

$$U_{compl-compl} = \frac{9Z^2(l)KTl_B}{4\pi(kR)^4}\left[\cosh - \frac{\sinh(kR)}{kR}\right]^2 \times \sum_{i=1}^{N-1}\left[\left[\frac{N-i}{i}\right]\frac{\exp\left(kD(N,l)\right)}{D(N,l)}\right] \qquad (19)$$

replace all terms in Equation (13), the total free energy of the system is written as:

$$\frac{U(N,l)}{K_B T} = \left\{ \frac{3}{4\pi} \frac{NZ(l) l_B A}{(kR)^2} \left[\frac{Z(l) e^{-kR}}{2R} + \frac{1}{b} \int_R^{L-Nl} \frac{e^{-kr}}{r} dr + \frac{3Z(l)A}{2(kR)^2} \sum_{i=1}^{N-1} X_i \left(\frac{N-i}{i} \right) \frac{e^{-kD(N,l)}}{D(n,l)} \right] + \frac{1}{b} \Omega(a)(1-\xi^{-1})(L-Nl) + \frac{Nl_p}{2R^2} l \right\} \quad (19)$$

Where

$$A = \cosh(kR) - \frac{\sinh(kR)}{kR} \quad (20)$$

And

$$\int_R^{L-Nl} \frac{e^{-KT}}{r} dr = \left[\ln(kr) - \sum_{n=0}^{\infty} \frac{(-1)^n * (kr)^{n+1}}{(n+1)!(n+1)} \right]_R^{L-Nl} \quad (21)$$

2.4 Software analysis

To perform these calculations, some computational software programs are used. The Qtgrace program version 5.6.0 (Winter, 2017) was used for graphing and analyzing some of the theoretical results. In the current work, the optimization method of the total free energy for a system of LPE chains interacting with penetrable spheres was carried out by using the mathematical program Maple version 2021.1, (Bernardin et al., 2021). In addition to the Get Data Digitizer program version 2.26.0.20 (Fedorov, 2013), was used to extract values of some graphs previous studies.

Chapter Three

Results And Discussion

3.1 Introduction

The concept of optimal length was used in this study as a quantitative measure of the degree of LPE chain wrapping around the dendrimer. There are pivotal findings that contribute significantly to this study; the impact of acetylation on the degree of PE wrapping length around the dendrimer, the number of condensed monomers on the dendrimer, and the number of turns folded around it. Additionally, acetylation has an impact on the creation of linkers between complexes, hence the structure of an LPE chain connected to several dendrimers has also been studied.

3.2 Computational details

By taking the first derivative of the total free energy equation for the penetrable sphere model (Eq. 3) with respect to the wrapping length l and equating it to zero (i.e., the total free energy equation has to be minimized). The optimal length (l_{opt}) of the LPE chain that has been wrapped around the dendrimer for a system of LPE chain and PAMAM dendrimer of different radii can be found by Maple 2021 software.

In this study the penetrable sphere model was used to study the electrostatic interaction free energy for a system composed of a charged sphere and an oppositely charged LPE chain. The dendrimer modeled EDA-core PAMAM dendrimer G5, as a sphere of radius R_s, and charge Z_d. The semiflexible LPE chains modeled as DNA with different contour lengths, L= 90 nm of 265 bp, L=184 nm of 541 bp and L=680 nm of 2000 bp. These lengths have persistence length lp and a space between bases b. The system is done at 1:1 salt concentration at 10mM corresponding to Debye screening length (DSL) with a Bjerum length of 0.71 nm at room temperature.

3.3 System of Single PAMAM dendrimer – LPE chain complex

3.3.1 Effect of Acetylation on single PAMAM dendrimer – LPE complex conformation.

Table 3.1: Properties of the PAMAM dendrimer (EDA) core of different radii, R_s, investigated by (Shi Yu, 2015), while the charge of the acetylated dendrimer Z_d, the surface charge density σ and the isoelectric length l_{iso} have been investigated by this study.

$Acetylation$ %	R_s (nm)	Z (e)	σ $(e.nm^{-2})$	l_{iso} for single strand (ss)	l_{iso} for Double strand (ds)
0	2.67	128.0	1.43	43.52	21.76
10	2.58	115.2	1.38	39.17	19.58
20	2.50	102.4	1.30	34.82	17.41
30	2.42	89.6	1.22	30.46	15.23
40	2.35	76.8	1.11	26.11	13.06
50	2.24	64.0	1.02	21.76	10.88
60	2.18	51.2	0.86	17.41	8.70
70	2.14	38.4	0.67	13.06	6.53
80	2.11	25.6	0.46	8.70	4.35
90	2.07	12.8	0.24	4.35	2.18

Table (3.1) The complexes' charges will be determined using the model of Shi Yu (Shi Yu, 2015). Determining the extent to which the DNA molecule is wrapped around a dendrimer will also be achievable. As revealed from this table, by increasing acetylation, the dendrimer radius R_s decreases and contracts. Consequently, the positive charge of the dendrimer is reduced. From these observations, we built up our results. The effect of acetylation on the R_s is reduced by 0.6 nm, and the charge is reduced by 115.2 e, as shown in Table (3.2).

Table 3.2: The amount of radius R_s and charge Z_d reduction caused by acetylation.

Acetylation%	R_s	Z_d
0	2.67	128
90	2.07	12.8

At different acetylation percentages, the complexation between a positively charged sphere and a negatively charged semi-flexible LPE chain has been studied. The system is composed of G5

PAMAM EDA-core as a sphere of different R_s and different Z_d (illustrated in Table 3.1), which is complexed with an oppositely charged semiflexible LPE chain of lp = 50 nm at a 1:1 salt concentration at 10 mM, corresponding to a DSL of 3 nm with a Bjerum length of 0.71 nm when number of dendrimers N = 1. Various PE chain lengths have been used (L = 90, 184, and 680 nm) with b = 0.34, which has been considered with the single strands, and b = 0.17 nm has been used with the double strands. Fig. (3.1) shows, for various LPE chain lengths predicted theoretically, the l_{opt} wrapping around dendrimers using the penetrable sphere model. Fig (3.1) shows that, according to Shi Yu (2015), raising the acetylation percentage results in a decrease in R_s, which in turn causes the l_{opt} to become less wrapped around the dendrimer for all PE chain lengths (single strands and double strands). When these findings are compared to those predicted by Qamhieh and colleagues (Qamhieh et al., 2022), it is shown that the optimal DNA wrapping length does indeed decrease with R_s.

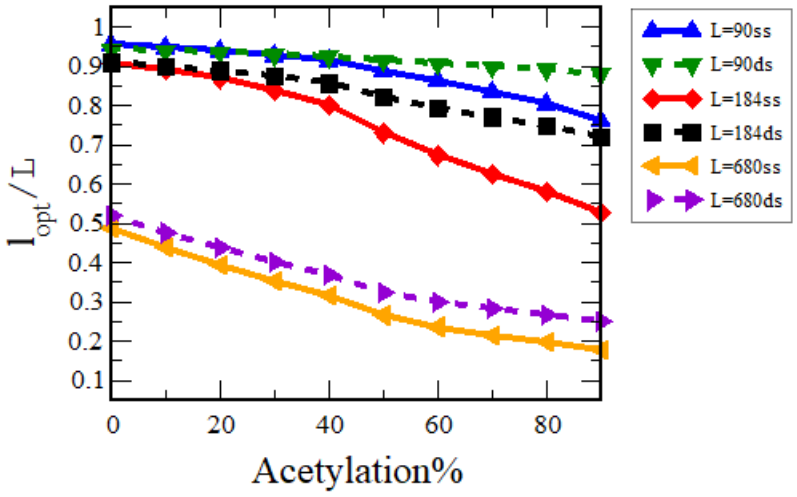

Figure 3.1: The ratio of l_{opt} to the length of PE as a function of acetylation %. (Solid lines for ss chains, and dashed lines for ds chains).

Based on the penetrable sphere model, Fig. (3.2) shows the number of condensed PE chain monomers on the dendrimer for various theoretically predicted LPE chain lengths. Fig (3.2) demonstrates that as the acetylation percentage is increased, the R_s shrinks, resulting in a decrease in the number of condensed PE chain monomers for both single-stranded and double-stranded PE chains. The dendrimer has a large curvature and a low surface charge density as a result of its radius

shrinking, which reduces the neutralization's impact on the electrostatic interaction. These results are in agreement with those of Qamhieh and co-workers (Qamhieh et al., 2014), who discovered that G2's larger curvature made neutralization less effective than for G6 or G8.

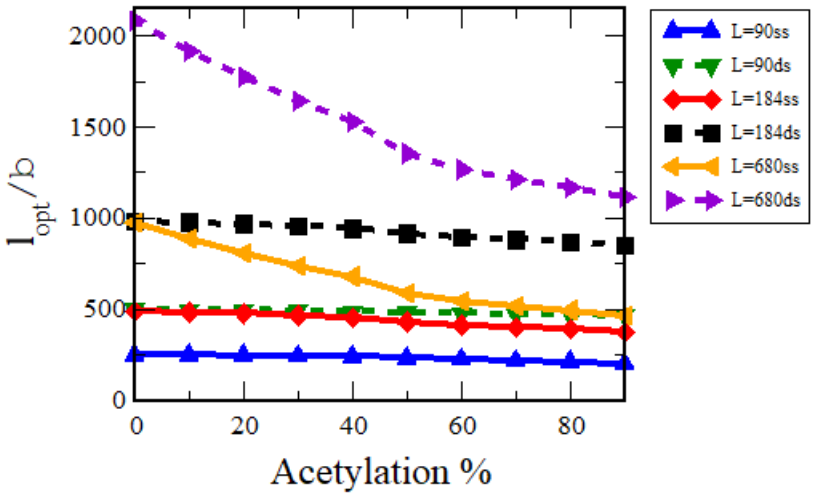

Figure 3.2: The number of condensed monomers as a function of acetylation %. (Solid lines for ss chains, and dashed lines for ds chains).

Now, the complex structure of an LPE chain and a single dendrimer has been investigated. Tables (3.3 – 3.8) show the effect of the reduction of the dendrimer size on the l_{opt} around the dendrimer, the total charge of the dendrimer-PE complex, and other structural properties of the complex. The results of the interaction are modeled as a function of the acetylated R_s. The difference between the optimal wrapped length and the length needed to neutralize the dendrimer charges $Diff\ (nm) = l_{opt} - l_{iso}$, $Z^* = Z_d + Z_{l_{opt}}$ is the charge of the complex which equal the charge of the dendrimer Z_d and the charge of the PE chain wrapping around the dendrimer $Z_{l_{opt}}$, the length needed to neutralize the dendrimer charges is $l_{iso} = Z_d b$, and the number of PE chain length turns around each dendrimer is considered as $l_{opt}/2\pi R_s$.

Table 3.3: The interaction between acetylated G5 dendrimer N=1 and LPE of chain length L = 90 nm, with ss when b=0.34 nm.

$Acetylation\%$	**0**	**10**	**20**	**30**	**40**	**50**	**60**	**70**	**80**	**90**
$R_s\ (nm)$	2.67	2.58	2.50	2.42	2.35	2.24	2.18	2.14	2.11	2.07
$lopt\ (nm)$	85.92	85.24	84.44	83.43	82.20	79.95	77.62	75.13	72.40	68.52
$Diff\ (nm)$	41.1	44.9	48.6	52.1	55.3	57.6	59.7	61.7	63.4	64.0
Z^*	-124.7	-135.5	-146.0	-155.8	-165.0	-171.1	-177.1	-182.6	-187.3	-188.7
Z^*/Z	-1.0	-1.2	-1.4	-1.7	-2.1	-2.7	-3.5	-4.8	-7.3	-14.7
$l_{opt}/2\pi R_s$	5.1	5.3	5.4	5.5	5.6	5.7	5.7	5.6	5.5	5.3

Table 3.4: The interaction between acetylated G5 dendrimer N=1 and LPE of chain length L = 90 nm, with ds when b=0.17 nm.

$Acetylation\%$	**0**	**10**	**20**	**30**	**40**	**50**	**60**	**70**	**80**	**90**
$R_s\ (nm)$	2.67	2.58	2.50	2.42	2.35	2.24	2.18	2.14	2.11	2.07
$lopt\ (nm)$	84.88	84.52	84.13	83.67	83.17	82.33	81.59	80.85	80.16	79.21
$Diff\ (nm)$	63.1	64.9	66.7	68.4	70.1	71.5	72.9	74.3	75.8	77.0
Z^*	-371.3	-382.0	-392.5	-402.6	-412.4	-420.3	-428.7	-437.2	-445.9	-453.1
Z^*/Z	-2.9	-3.3	-3.8	-4.5	-5.4	-6.6	-8.4	-11.4	-17.4	-35.4
$l_{opt}/2\pi R_s$	5.1	5.2	5.4	5.5	5.6	5.8	6.0	6.0	6.0	6.1

Table 3.5: The interaction between acetylated G5 dendrimer N=1 and LPE of chain length L = 184 nm, with ss when b=0.34 nm.

$Acetylation\%$	**0**	**10**	**20**	**30**	**40**	**50**	**60**	**70**	**80**	**90**
$R_s\ (nm)$	2.67	2.58	2.50	2.42	2.35	2.24	2.18	2.14	2.11	2.07
$lopt\ (nm)$	166.80	164.79	162.30	159.00	155.30	147.00	141.00	136.90	133.30	128.30
$Diff\ (nm)$	123.3	125.6	127.5	128.5	129.2	125.2	123.6	123.8	124.6	123.9
Z^*	-362.6	-369.5	-375.0	-378.0	-380.0	-368.4	-363.5	-364.2	-366.5	-364.6
Z^*/Z	-2.8	-3.2	-3.7	-4.2	-4.9	-5.8	-7.1	-9.5	-14.3	-28.5
$l_{opt}/2\pi R_s$	9.9	10.2	10.3	10.5	10.5	10.4	10.3	10.2	10.1	9.9

Table 3.6: The interaction between acetylated G5 dendrimer N=1 and LPE of chain length L = 184 nm, with ds when b=0.17 nm.

$Acetylation\%$	**0**	**10**	**20**	**30**	**40**	**50**	**60**	**70**	**80**	**90**
$R_s\ (nm)$	2.67	2.58	2.50	2.42	2.35	2.24	2.18	2.14	2.11	2.07
$lopt\ (nm)$	167.30	166.00	164.50	162.70	160.30	155.70	152.40	149.77	147.60	144.40
$Diff\ (nm)$	145.5	146.4	147.1	147.5	147.2	144.8	143.7	143.2	143.2	142.2
Z^*	-856.1	-861.3	-865.2	-867.5	-866.1	-851.9	-845.3	-842.6	-842.6	-836.6
Z^*/Z	-6.7	-7.5	-8.4	-9.7	-11.3	-13.3	-16.5	-21.9	-32.9	-65.4
$l_{opt}/2\pi R_s$	10.0	10.2	10.5	10.7	10.9	11.1	11.1	11.1	11.1	11.1

Table 3.7: The interaction between acetylated G5 dendrimer N=1 and LPE of chain length L = 680 nm, with ss when b=0.34 nm.

$Acetylation\%$	**0**	**10**	**20**	**30**	**40**	**50**	**60**	**70**	**80**	**90**
$R_s\ (nm)$	2.67	2.58	2.50	2.42	2.35	2.24	2.18	2.14	2.11	2.07
$lopt\ (nm)$	330.00	300.50	275.19	250.88	230.50	200.50	185.00	175.00	167.90	158.57
$Diff\ (nm)$	286.5	261.3	240.4	220.4	204.4	178.7	167.6	161.9	159.2	154.2
Z^*	-842.6	-768.6	-707.0	-648.3	-601.1	-525.7	-492.9	-476.3	-468.2	-453.6
Z^*/Z	-6.6	-6.7	-6.9	-7.2	-7.8	-8.2	-9.6	-12.4	-18.3	-35.4
$l_{opt}/2\pi R_s$	19.7	18.5	17.5	16.5	15.6	14.2	13.5	13.0	12.7	12.2

Table 3.8: The interaction between acetylated G5 dendrimer N=1 and LPE of chain length L = 680 nm, with ds when b=0.17 nm.

$Acetylation\%$	**0**	**10**	**20**	**30**	**40**	**50**	**60**	**70**	**80**	**90**
$R_s\ (nm)$	2.67	2.58	2.50	2.42	2.35	2.24	2.18	2.14	2.11	2.07
$lopt\ (nm)$	353.40	325.60	301.70	278.50	259.10	230.20	215.30	205.69	198.65	189.50
$Diff\ (nm)$	331.6	306.0	284.3	263.3	246.0	219.3	206.6	199.2	194.3	187.3
Z^*	-1950.8	-1800.1	-1672.3	-1548.6	-1447.3	-1290.1	-1215.3	-1171.5	-1142.9	-1101.9
Z^*/Z	-15.2	-15.6	-16.3	-17.3	-18.8	-20.2	-23.7	-30.5	-44.6	-86.1
$l_{opt}/2\pi R_s$	21.1	20.1	19.2	18.3	17.5	16.4	15.7	15.3	15.0	14.6

According to Table (3.3), when the R_s is decreased by acetylation, the l_{opt} of PE chain wrapping around the G5 PAMAM dendrimer of EDA core significantly decreased from 85.92 to 68.52. As a result, the difference $Diff$ increased. The Z^* is always negative, which means that the dendrimer's charge is inverted and is increasingly negatively charged as the radius decreases. The complex's charge inversion ratio increases (negative charge increases). It was discovered that the ratio between the circumference of the complex and the l_{opt} was set at about 5.5.

From Table (3.4), when the R_s is decreased by acetylation, the l_{opt} wrapping around the G5 PAMAM dendrimer of EDA-core drastically dropped from 84.88 to 79.21. As a result, the $Diff$ widens. The Z^* has always been negative, making the charge of the dendrimer inverts and it becomes increasingly negatively charged as the radius decreases. The complex charge inversion ratio increases (negative charge increases). By decreasing the radius of the dendrimer, the ratio between the complex circumference and the l_{opt} was shown to slightly increase, which is considered roughly constant.

According to Table (3.5), when the R_s decreased by acetylation, the l_{opt} wrapping around the G5 PAMAM dendrimer of EDA core dramatically dropped from 166.80 to 128.30. As a result, the $Diff$ is increased until it reaches 40%, at this point it begins to vary. The Z_d is inverted because the net charge of the complex is negative for all values. And it increases from 0% acetylation to 40%, after that the complex's charge starts to vary. The charge inversion ratio of the PE-G5 dendrimer has a negative value for all radius sizes and increases with decreasing radius size. Also, we can find that the charge inversion value is closest to neutralizing at zero acetylation. It was discovered that the ratio of the complex circumference to the l_{opt} was nearly constant.

Table (3.6) reveals that when the R_s is reduced by acetylation, the optimal DNA wrapping length around the G5 PAMAM dendrimer of EDA- core drastically decreased from 167.30 to 144.40. As a result, the $Diff$ increases until it reaches 30%, thereafter it starts to decrease until it reaches 90%. We find that the Z_d is inverted because the complex net charge is always negative. The Z^* begins to rise until it reaches 30%, at which point it begins to fall until 90%, all while shrinking in radius. The charge inversion ratio of PE-dendrimer G5 complex is raised (an increase in negative charge).

It was observed that the ratio of the complex's circumference to its l_{opt} slightly increase until its radius reached 2.35 nm by acetylation, then it started to be quite steady.

Table (3.7) demonstrates that when R_s is reduced by acetylation, the l_{opt} wrapping around the G5 PAMAM dendrimer of EDA core markedly decreased from 330.00 to 158.57. The $Diff$ decreased as a consequence. The Z_d is always inverted since the Z^* is always negative. But by shrinking the radius, the dendrimer's charge is made less negatively charged. The PE-dendrimer G5 charge inversion ratio increases (negative charge increases) by decreasing R_s. It was found that the ratio between the circumference of the complex and the l_{opt} had fallen from 19.7 to 12.2.

Table (3.8) which is the final table for explaining the properties of PE interaction with a single G5 dendrimer, shows that when the R_s is reduced by acetylation, the l_{opt} wrapping around a G5 dendrimer with an EDA core significantly decreased from 353.40 to 189.50. As a result, the $Diff$ decreases. The Z^* is negative, which indicates that the Z_d is inverted and reduced by shrinking the radius. The complex charge inversion ratio increases in negative charge by decreasing R_s. It was revealed that the ratio between the circumference of the complex and the l_{opt} decreased from 21.1 to14.6.

A comparison between the study findings and others was made (Qamhieh et al., 2014) using a DNA contour length of 1472.5 nm with the dendrimer of G4 with a different radius. This was done to analyze the findings obtained by the penetrable sphere model for the interaction between DNA molecules with different lengths (L = 90, 184, and 680 nm) and dendrimers of different radii as presented in Tables (3.3 - 3.8).

In our study, we found that the l_{opt} for all chain lengths used in the case of ss and ds decreased significantly irrespective of dendrimer contracts, as shown in Fig. (3.3), which is in accordance with what was obtained by Qamhieh and colleagues' (Qamhieh et al., 2014), in their study, which showed that the optimal wrapping length decreased by decreasing the dendrimer radius.

In addition, the $Diff$ in our study for complexes using 90 nm in the case of both ss and ds is significantly increased with decreasing R_s, which contradicts what Qamhieh and colleagues' (Qamhieh et al., 2014) showed that the difference is decreased by decreasing dendrimer radius.

For complexes using a length of 184 nm with different R_s, the $Diff$ is increased by decreasing R_s just for cases when dendrimer is acetylated from 0 to 30 %, which is also in contrast to what was obtained by Qamhieh and colleagues' results (Qamhieh et al., 2014). But it was in accordance with theirs in case the dendrimer is acetylated above 30 %, when the $Diff$ starts to decrease above this percentage by decreasing the R_s.

Finally, for complexes using a length of 680 nm, the $Diff$ agrees with Qamhieh and colleagues' findings (Qamhieh et al., 2014), except for the point when the dendrimer radius is at 100% acetylation, when the $Diff$ returns to increase slightly. Also, as illustrated in Fig. (3.4), we have shown that the Z^* of the complexes with lengths of 90 nm in the case of both ss and ds with all acetylated dendrimers is negative and increases in negativity by decreasing R_s, while for the complexes using lengths of 184 nm with both ss and ds, all have negative charges and significantly increase in negativity by decreasing R_s from zero to 30 % acetylation. This is in contrast to what was obtained by Qamhieh and colleagues' (Qamhieh et al., 2014), who showed that the net charge of complexes changes from negative to positive when dendrimer radius is decreased, which only agrees with the complexes using a length of 184 nm in the case of ss and ds, which decrease in their negative charges for all dendrimer acetylated above 30 %, and agree with complexes using 680 nm with acetylated dendrimer.

The number of turns wrapping around the dendrimer with its different radii is nearly fixed by decreasing the R_s for complexes using lengths of 90 nm in the case of ss. While in the case of ds, the number of turns increases significantly, as Qamhieh and colleagues'prove (Qamhieh et al., 2014).

For complexes using 184 nm in the case of ss and ds with dendrimer radii acetylated from 50 % to 90%, the number of turns is approximately fixed. But below these percentages, the number of turns increases by decreasing R_s until acetylation reaches 40%, which according to Qamhieh and colleagues' (Qamhieh et al., 2014), showed that the number of turns wrapping around the dendrimer

is increased by decreasing R_s. While for complexes using 680 nm in the case of ss and ds, the number of turns around the dendrimer is decreased by decreasing the R_s, in contrast with Qamhieh and colleagues' findings (Qamhieh et al., 2014). Number of turns on the dendrimer around LPE chain illustrated in Fig. (3.5).

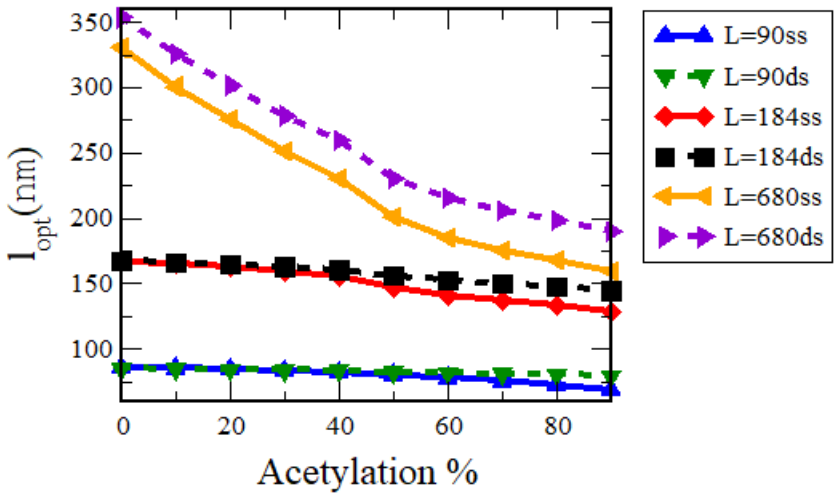

Figure 3.3: l_{opt} as a function of acetylation %, when N=1. Solid lines for ss chains, and dashed lines for ds chains.

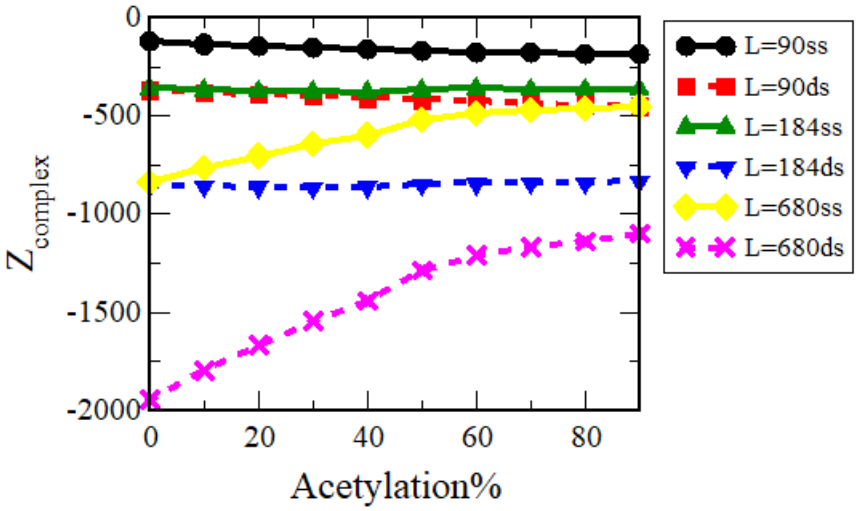

Figure 3.4: The net charge of the complex Z^* ($Z_{complex}$) as a function of acetylation %, when N=1. Solid lines for ss chains, and dashed lines for ds chains.

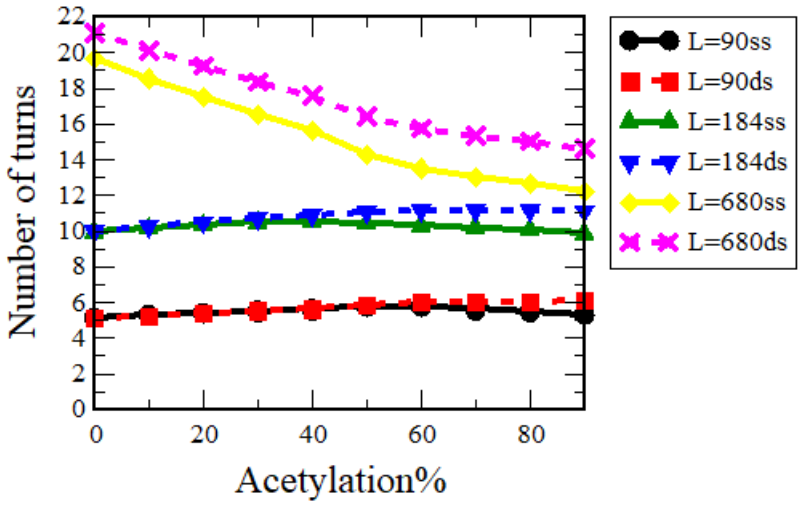

Figure 3.5: Number of turns on the dendrimer around LPE chain as a function of acetylation %, when N=1. Solid lines for ss chains, and dashed lines for ds chains.

3.4 System of multiple PAMAM dendrimers – LPE chain complexes

3.4.1 Effect of Acetylation on multiple PAMAM dendrimers – LPE complex conformation.

The total length of LPE is divided into two parts: the optimal wrapping length l_{opt} and the linker. Therefore, the effect of acetylation on the l_{opt} around dendrimer N and on the linker formed between complexes has been studied. The used system is composed of dendrimers when N = 2, 3, 4, 5, and 6, were modeled as EDA-core PAMAM dendrimers G5 as acetylated spheres with different percentages %, different R_s, and different Z_d (illustrated in Table (3.1)). Semiflexible LPE chain lengths of 184 and 680 nm were used for figures 3.5 and 3.6, respectively. This PE has a l_p of 50 nm and a b = 0.34 nm for the ss and b = 0.17 nm for the ds. The system is done at a 1:1 salt concentration, corresponding to a DSL of 3 nm with a Bjerum length of 0.71 nm.

Based on the data shown in Table (3.1), we can see that the R_s will decrease as the acetylation percentage increases, causing the dendrimer to become smaller and more compact. This compaction led to the discovery of a larger curvature, which implies less neutralization, which will decrease the

binding between the dendrimer and PE chain, as proven by Qamhieh et al. (Qamhieh et al., 2014). As a result, with regard to Fig. (3.6) and Fig. (3.7), we can observe that the l_{opt} wrapping around the dendrimer will shorten as the dendrimer becomes more compact, while the linker will increase greatly.

Furthermore, we can see that as the number of these dendrimers increases, the l_{opt} wrapping around them decreases, and the linker also gets shorter. This is in accordance with the findings of Qamhieh and coworkers (Qamhieh et al., 2009), who investigated the complexation of G4 dendrimers with DNA for two different DNA contour lengths and discovered that the system with a greater number of particles has a lower linker length than the system with fewer dendrimers bond to DNA.

Moreover, because the l_{opt} decreased as the number of dendrimers increased, it was discovered that the ss chain faced this decrease more than the ds chain at higher acetylation percentages in relation to increasing the number of dendrimers. This is because at higher acetylation percentages, the dendrimer radius decreases that the ss chain would not be able to overcharge dendrimers as much as the ds chain, which is considered more effective in neutralizing and overcharging dendrimers due to its higher negative charges. On the other hand, we found that when the degree of l_{opt} is higher in the case of using the ds chain than in the case of the ss chain, the linker length between complexes is shorter than the linker length in the case of the ss chain. And vice versa, when the degree of l_{opt} is higher in the case of using ss chain, longer linker length was found in the case of using ds chain.

For complexes using length of 184 nm with N = 5 and 6, we note that the l_{opt} of the ss chain starts to wrap at 20% and 30% acetylation, respectively. This is because at low acetylation %, the dendrimers' radii are larger. Indeed, using multiple dendrimers requires more negative charges for neutralizing and wrapping as revealed in Qamhieh and coworkers' studies (Qamhieh et al., 2009). They show that the degree of l_{opt} wrapped around the dendrimer particles with the higher N is less than the degree of l_{opt} wrapped around the dendrimer particles with the lower N.
From Fig. (3.6) and Fig. (3.7), we conclude that by increasing acetylation %, the longer chain length of 680 nm with the ds chain, gives us better overcharging with dendrimers for most dendrimer radii than the shorter length of 184 nm.

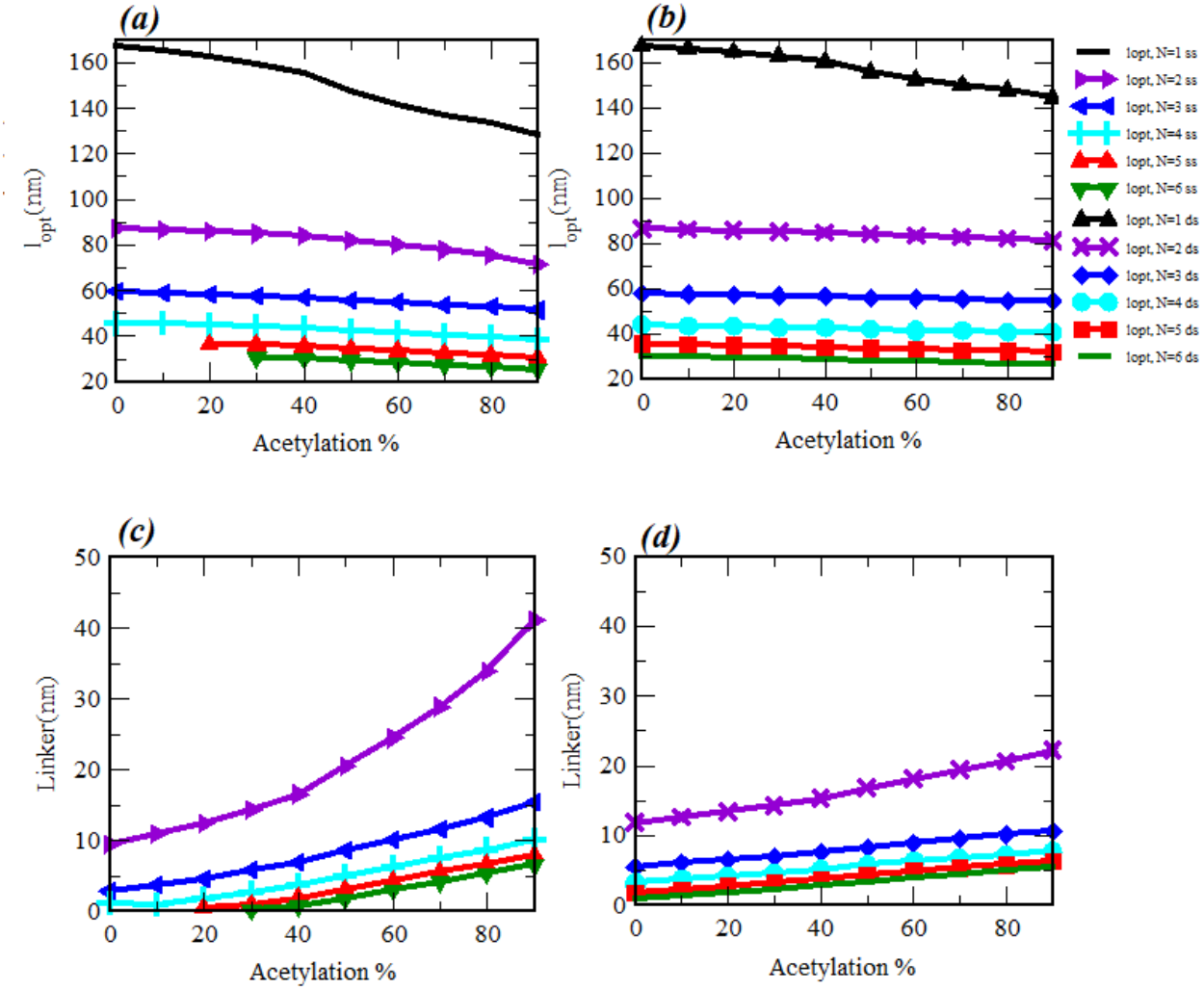

Figure 3.6: l_{opt} and Linker formed between G5 complexes with an oppositely charged semiflexible LPE as a function of acetylation %. The LPE chain length used, L=184 nm. (a) and (c) for ss b=0.34, (b) and (d) for ds b=0.17.

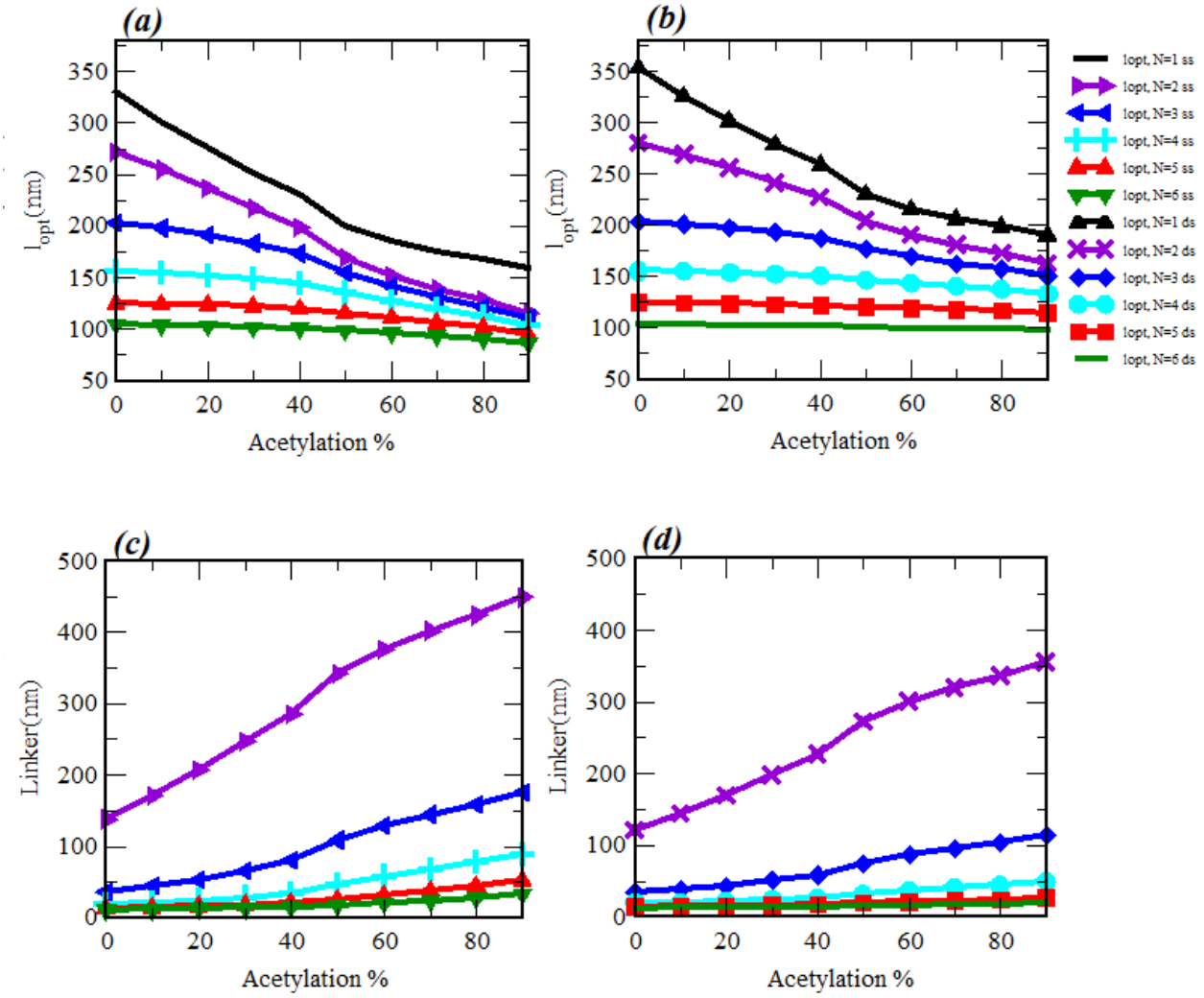

Figure 3.7: l_{opt} and Linker formed between G5 complexes with an oppositely charged semiflexible LPE as a function of acetylation %. The LPE chain length used, L=680 nm. (a) and (c) for ss b=0.34, (b) and (d) for ds b=0.17.

As mentioned before, acetylation of dendrimers affects their size and their charge. Therefore, this in turn affects the structural properties of LPE-dendrimer complexes when we have more than one dendrimer. The structural properties of LPE-dendrimer complexes have been studied when N=2. Tables (3.9 –3.14) show the effect of the reduction of the acetylated dendrimer size on the l_{opt} of PE chain around the dendrimer, the total charge of the dendrimer and PE complex, and other structural properties of the complexes. The results of the interaction are modeled as a function of

R_s, $Diff$, Z^*, $l_{opt}/2\pi R_s$, and the length of the LPE chain linking two neighboring dendrimers is given by $Linker\ (nm) = (L - N(lopt))/(N - 1)$.

Table 3.9: The interaction between acetylated G5 dendrimers N=2 and LPE of chain length L = 90 nm, with ss when b=0.34 nm.

$\boldsymbol{Acetylation\%}$	**0**	**10**	**20**	**30**	**40**	**50**	**60**	**70**	**80**	**90**
$\boldsymbol{R_s\ (nm)}$	2.67	2.58	2.50	2.42	2.35	2.24	2.18	2.14	2.11	2.07
$\boldsymbol{lopt\ (nm)}$	44.60	44.33	44.05	43.55	42.95	41.18	41.35	40.50	39.60	38.46
$\boldsymbol{Diff\ (nm)}$	1.1	5.2	9.2	13.1	16.8	19.4	23.9	27.4	30.9	34.1
$\boldsymbol{Z^*}$	-3.2	-15.2	-27.2	-38.5	-49.5	-57.1	-70.4	-80.7	-90.9	-100.3
$\boldsymbol{Z^*/Z}$	0.0	-0.1	-0.3	-0.4	-0.6	-0.9	-1.4	-2.1	-3.5	-7.8
$\boldsymbol{Linker\ (nm)}$	0.8	1.3	1.9	2.9	4.1	7.6	7.3	9.0	10.8	13.1
$\boldsymbol{l_{opt}/2\pi R_s}$	2.7	2.7	2.8	2.9	2.9	2.9	3.0	3.0	3.0	3.0

Table 3.10: The interaction between acetylated G5 dendrimers N=2 and LPE of chain length L = 90 nm, with ds when b=0.17 nm.

$\boldsymbol{Acetylation\%}$	**0**	**10**	**20**	**30**	**40**	**50**	**60**	**70**	**80**	**90**
$\boldsymbol{R_s}$	2.67	2.58	2.50	2.42	2.35	2.24	2.18	2.14	2.11	2.07
$\boldsymbol{lopt\ (nm)}$	43.25	43.04	42.80	42.53	42.26	41.90	41.58	41.25	40.95	40.60
$\boldsymbol{Diff\ (nm)}$	21.5	23.5	25.4	27.3	29.2	31.0	32.9	34.7	36.6	38.4
$\boldsymbol{Z^*}$	-126.4	-138.0	-149.4	-160.6	-171.8	-182.5	-193.4	-204.2	-215.3	-226.0
$\boldsymbol{Z^*/Z}$	2.0	2.2	2.5	2.8	3.2	3.9	4.8	6.3	9.4	18.7
$\boldsymbol{Linker\ (nm)}$	3.5	3.9	4.4	4.9	5.5	6.2	6.8	7.5	8.1	8.8
$\boldsymbol{l_{opt}/2\pi R_s}$	2.6	2.7	2.7	2.8	2.9	3.0	3.0	3.1	3.1	3.1

Table 3.11: The interaction between acetylated G5 dendrimers N=2 and LPE of chain length L = 184 nm, with ss when b=0.34 nm.

$Acetylation\%$	**0**	**10**	**20**	**30**	**40**	**50**	**60**	**70**	**80**	**90**
$R_s\ (nm)$	2.67	2.58	2.50	2.42	2.35	2.24	2.18	2.14	2.11	2.07
$lopt\ (nm)$	87.33	86.61	85.81	84.86	83.75	81.80	79.80	77.58	75.10	71.50
$Diff\ (nm)$	87.3	76.6	65.8	54.9	43.8	31.8	19.8	7.6	-4.9	-18.5
Z^*	-67.3	-46.6	-25.8	-4.9	16.3	38.2	60.2	82.4	104.9	18.5
Z^*/Z	-1.0	-1.2	-1.5	-1.8	-2.2	-2.8	-3.6	-4.9	-7.6	-15.4
$Linker\ (nm)$	9.3	10.8	12.4	14.3	16.5	20.4	24.4	28.8	33.8	41.0
$l_{opt}/2\pi R_s$	5.2	5.3	5.5	5.6	5.7	5.8	5.8	5.8	5.7	5.5

Table 3.12: The interaction between acetylated G5 dendrimers N=2 and LPE of chain length L = 184 nm, with ds when b=0.17 nm.

$Acetylation\%$	**0**	**10**	**20**	**30**	**40**	**50**	**60**	**70**	**80**	**90**
$R_s\ (nm)$	2.67	2.58	2.50	2.42	2.35	2.24	2.18	2.14	2.11	2.07
$lopt\ (nm)$	86.10	85.72	85.32	84.87	84.39	83.61	82.96	82.34	81.72	80.91
$Diff\ (nm)$	-64.3	-66.1	-67.9	-69.6	-71.3	-72.7	-74.3	-75.8	-77.4	-78.7
Z^*	-378.5	-389.0	-399.5	-409.6	-419.6	-427.8	-436.8	-446.0	-455.1	-463.1
Z^*/Z	-3.0	-3.4	-3.9	-4.6	-5.5	-6.7	-8.5	-11.6	-17.8	-36.2
$Linker\ (nm)$	11.8	12.6	13.4	14.3	15.2	16.8	18.1	19.3	20.6	22.2
$l_{opt}/2\pi R_s$	5.1	5.3	5.4	5.6	5.7	5.9	6.1	6.1	6.2	6.2

Table 3.13: The interaction between acetylated G5 dendrimers N=2 and LPE of chain length L = 680 nm, with ss when b=0.34 nm.

$Acetylation\%$	**0**	**10**	**20**	**30**	**40**	**50**	**60**	**70**	**80**	**90**
$R_s\ (nm)$	2.67	2.58	2.50	2.42	2.35	2.24	2.18	2.14	2.11	2.07
$lopt\ (nm)$	279.64	268.25	255.71	241.17	226.9	203.9	190.1	180.23	172.3	162.4
$Diff\ (nm)$	-257.9	-248.7	-238.3	-225.9	-213.8	-193.0	-181.4	-173.7	-167.9	-160.2
Z^*	-1516.9	-1462.7	-1401.8	-1329.0	-1257.9	-1135.4	-1067.0	-1021.8	-987.9	-942.5
Z^*/Z	-11.9	-12.7	-13.7	-14.8	-16.4	-17.7	-20.8	-26.6	-38.6	-73.6
$Linker\ (nm)$	120.7	143.5	168.6	197.7	226.2	272.2	299.8	319.5	335.4	355.2
$l_{opt}/2\pi R_s$	16.7	16.5	16.3	15.9	15.4	14.5	13.9	13.4	13.0	12.5

Table 3.14: The interaction between acetylated G5 dendrimers N=2 and LPE of chain length L = 680 nm, with ds when b=0.17 nm.

$\boldsymbol{Acetylation}\%$	**0**	**10**	**20**	**30**	**40**	**50**	**60**	**70**	**80**	**90**
$\boldsymbol{R_s\ (nm)}$	2.67	2.58	2.50	2.42	2.35	2.24	2.18	2.14	2.11	2.07
$\boldsymbol{lopt\ (nm)}$	271.02	254.60	236.85	216.95	198.00	169.40	152.00	139.10	128.45	115.76
$\boldsymbol{Diff\ (nm)}$	-227.5	-215.4	-202.0	-186.5	-171.9	-147.6	-134.6	-126.0	-119.7	-111.4
$\boldsymbol{Z^*}$	-669.1	-633.6	-594.2	-548.5	-505.6	-434.2	-395.9	-370.7	-352.2	-327.7
$\boldsymbol{Z^*/Z}$	-5.2	-5.5	-5.8	-6.1	-6.6	-6.8	-7.7	-9.7	-13.8	-25.6
$\boldsymbol{Linker\ (nm)}$	138.0	170.8	206.3	246.1	284.0	341.2	376.0	401.8	423.1	448.5
$\boldsymbol{l_{opt}/2\pi R_s}$	16.2	15.7	15.1	14.3	13.4	12.0	11.1	10.3	9.7	8.9

According to Table (3.9), when the R_s is decreased by acetylation, the l_{opt} of PE chain wrapping around the G5 PAMAM dendrimer of EDA core significantly decreased from 44.60 to 38.46. As a result, the $Diff$ expands. The $Z^*$is negative for all values. Therefore, the Z_d is inverted, and as the radius decreases, it becomes more negatively charged. The PE- dendrimer G5 charge inversion ratio increases in negative charge by decreasing R_s. It was discovered that by increasing acetylation, which results in a reduction in radius size, the linker between complexes increased from 0.8 to 13.1. It was reported that the ratio of the complex circumference to the l_{opt} was relatively constant at roughly 2.9.

From Table (3.10), the l_{opt} wrapping around G5 PAMAM dendrimer of EDA core decreased significantly from 43.25 to 40.60 when the dendrimer radius was decreased by acetylation. As a result, the $Diff$ increased. The Z^* is negative for all values, and that means that the charge of the dendrimer is inverted. And the charge inversion ratio of the complex increases. Nevertheless, it was discovered that increasing acetylation, which results in a reduction in radius size, increased the linker between complexes from 3.5 to 8.8. It was observed that the ratio between the circumference of the complex and the l_{opt} increased slightly, which is considered roughly constant.

From Table (3.11), when the dendrimer radius was shrunk by acetylation, the l_{opt} wrapping around the G5 PAMAM dendrimer of EDA core decreased dramatically from 87.33 to 71.5. Up to 70% acetylation, the $Diff$ became less. The resulting values then turns negative for 80 and 90% acetylation as a result of the dendrimer of G5 not being fully neutralized by the LPE with the

opposite charge. The Z_d is reversed because the Z^* was negative from the beginning of acetylation until 30%. From 40% to 90% acetylation, the charge then turns positive. The G5 dendrimer in this instance totally inverts the charge of the PE. PE chain becomes completely neutralized, as well. These findings highlight the significance of the charge inversion in gene transport due to the negatively charged cell membrane. The charge inversion ratio of the complex was increased in negative charge by dendrimer contraction. Furthermore, it was discovered that by increasing acetylation, which results in a reduction in radius size, the linker between complexes increased dramatically from 9.3 to 41.0. The l_{opt} to complex circumference ratio was found to be set at about 5.

Table (3.12) demonstrates when R_s is reduced by acetylation, the l_{opt} around the G5 PAMAM dendrimer of EDA core significantly decreases from 86.10 to 80.91. As a result, the $Diff$ has a negative charge for all values. The negative charge implies that the dendrimer of G5 is partially neutralized by the oppositely charged PE. The Z^* is negative and increases as the R_s decreases. This means that the Z_d is inverted upon the interaction between the LPE chain and the dendrimer. However, it was observed that the linker between complexes increased from 11.8 to 22.0. When dendrimer radius is decreased, it was shown that the ratio between the l_{opt} and the complex circumference increased slightly, which is considered approximately constant.

Table (3.13) shows when R_s is shrunk by acetylation, the l_{opt} wrapping around the G5 PAMAM dendrimer of EDA core significantly decreases. As a result, the $Diff$ decreased in negative charge. The negative charge implies that the dendrimer of G5 is partially neutralized by the oppositely charged PE. The Z^* is always negative. This means that the Z_d is reversed due to the interaction between the LPE chain and the dendrimer, and it is decreased by increasing acetylation and reducing the radius of the dendrimer. Furthermore, it was discovered that by increasing acetylation, which results in a reduction in radius size, the linker between complexes increased from 120.7 to 355.2. When dendrimer radius is reduced, it was revealed that the ratio between the l_{opt} and the circumference of the complex falls from 16.7 to 12.5.

According to Table (3.14), when the dendrimer radius is reduced by acetylation, the l_{opt} wrapping around the G5 PAMAM dendrimer of EDA core decreases significantly. As a consequence, the

$Diff$ length decreased in negative charge. The negative values imply that the dendrimer of G5 is partially neutralized by the oppositely charged PE. By raising the acetylation percentage, the Z^* is increased in the negative charge, which means that the Z_d is reversed due to the interaction between the LPE chain and the dendrimer. As a result, the value of the charge inversion increases in negative charge. Furthermore, it was found that by increasing the acetylation percentage, which causes a decrease in radius size, the linker between complexes increased considerably from 138.0 to 448.5. When dendrimer radius is reduced, it was discovered that the ratio between the l_{opt} and the circumference of the complex falls from 16.2 to 8.9.

A comparison between the obtained results and other findings was made by Qamhieh and colleagues (Qamhieh et al., 2009; Qamhieh et al., 2014) to summarize the results of the penetrable sphere model for the interaction of DNA molecules with different chain lengths (L = 90, 184, and 680 nm) and dendrimers of different radii as shown in Tables (3.9) through Table (3.14).We found that the l_{opt} for all chain lengths used, in the case of ss and ds, decreased significantly despite the decrease in the R_s, as shown in Fig. (3.8), which is in accordance with what was obtained by Qamhieh and associates in their study (Qamhieh et al., 2009; Qamhieh et al., 2014), which showed that the l_{opt} decreased by decreasing the dendrimer radius.

In addition, the $Diff$ in our study for complexes using 90 nm, in the case of both ss and ds, is significantly increased with decreasing R_s, which is in contrast to what Qamhieh had found (Qamhieh et al., 2009; Qamhieh et al., 2014), who showed that the difference is decreased by decreasing R_s from positive to negative. On the other hand, our results are in accordance with theirs for the complexes that used lengths of 184 and 680 nm for both ss and ds, where the $Diff$ decreased with decreasing R_s.

Also, we have shown that the net charge of the complexes with lengths of 90 and 184 nm of both ss and ds, is negative and increases in negativity by decreasing R_s, as illustrated in Fig. (3.9). This was found to be in contrast to Qamhieh and associates concluded. They showed that by decreasing R_s, the Z^*decreases in negativity and goes from negative to positive. On the other hand, our results for the complexes using length of 680 nm in the case of ss and ds, showed that the net charge of the complexes decreased in its negative charge by decreasing R_s. This agrees with Qamhieh and associates' findings (Qamhieh et al., 2009; Qamhieh et al., 2014), since their Z^* results changed from negative to positive.

Furthermore, we showed that the linker between complexes for all chain lengths used increased when dendrimers decreased in radii. This agrees with Qamhieh and associates' studies (Qamhieh et al., 2009; Qamhieh et al., 2014), which revealed that the linker increases with the decrease of dendrimer radius.

The number of turns of PE wrapping around dendrimers is illustrated in Fig. (3.10), and from this figure, the number of turns is slightly constant for complexes using the lengths of 90 and 184 nm, in the case of ss and ds, by decreasing R_s. These findings are in contrast with Qamhieh and associates' findings (Qamhieh et al., 2009; Qamhieh et al., 2014), which showed that the number of turns increases with decreasing dendrimer radius. While for complexes using the length of 680 nm for both ss and ds, the number of turns wrapping around the dendrimer is decreased by the dendrimer's decrease in radius, which goes in contrast to Qamhieh and associates' results (Qamhieh et al., 2009; Qamhieh et al., 2014).

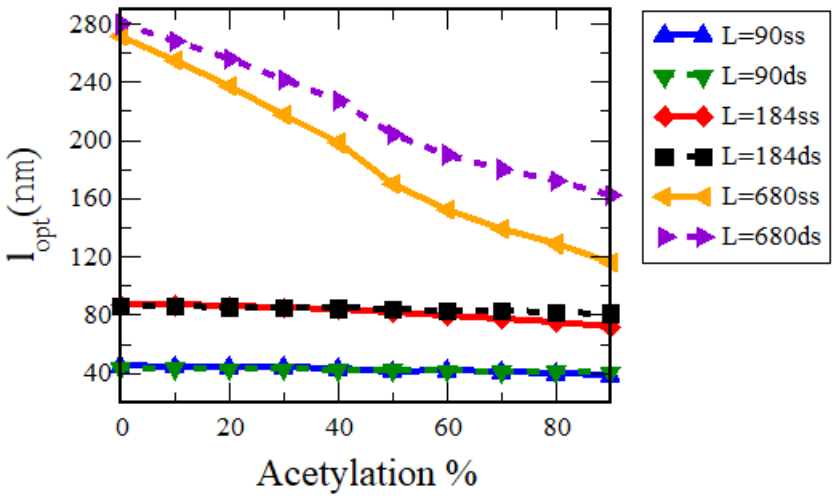

Figure 3.8: l_{opt} as a function of acetylation %, when N=2. Solid lines for ss chains, and dashed lines for ds chains.

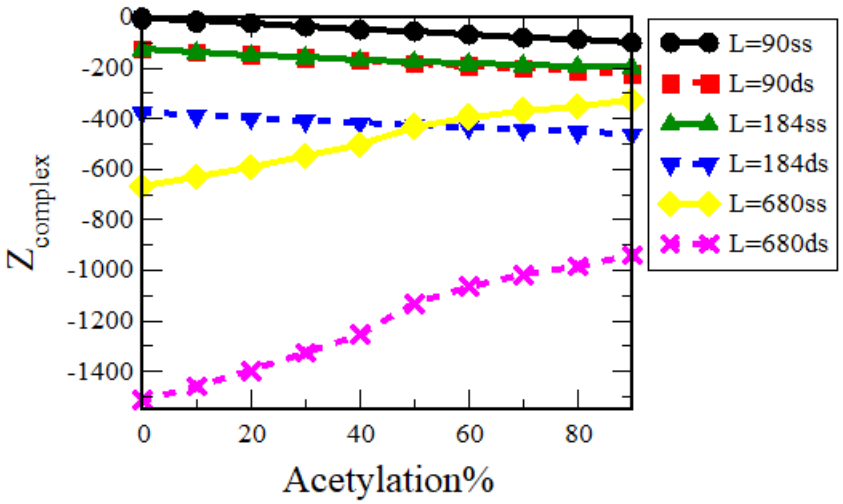

Figure 3.9: The net charge of the complex Z^* ($Z_{complex}$) as a function of acetylation %, when N=2. Solid lines for ss chains, and dashed lines for ds chains.

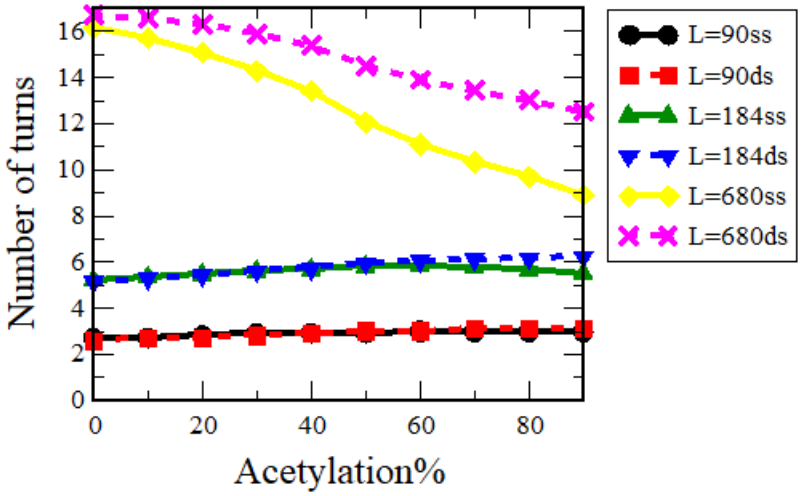

Figure 3.10: Number of turns on the dendrimer around LPE chain as a function of acetylation %, when N=2. (Solid lines for ss chains, and dashed lines for ds chains).

To demonstrate the change in the net charge of complexes with more than two dendrimers, Fig. (3.11) shows that the net charge of complexes with a length of 184 nm of both ss and ds chains is negative and increases in negativity as acetylation increases. For the complexes with a length of 680 nm, the net charge of the complexes is negative and decreases in negativity when using dendrimers of N = 3 and 4 in the case of ss and ds chains, except when using ss chains with N = 4, where a small

increase in negative charge was found by increasing acetylation. In addition, when using N = 5 with the ss and ds chains, the net charge of the complex is negative and increases in negativity, similar to the complexes using N = 6 with the ds chain. On the other hand, when using N = 6 with the ss chain, the net charge of the complex is positive and increases in positivity by increasing acetylation, except at zero acetylation, where it is negative.

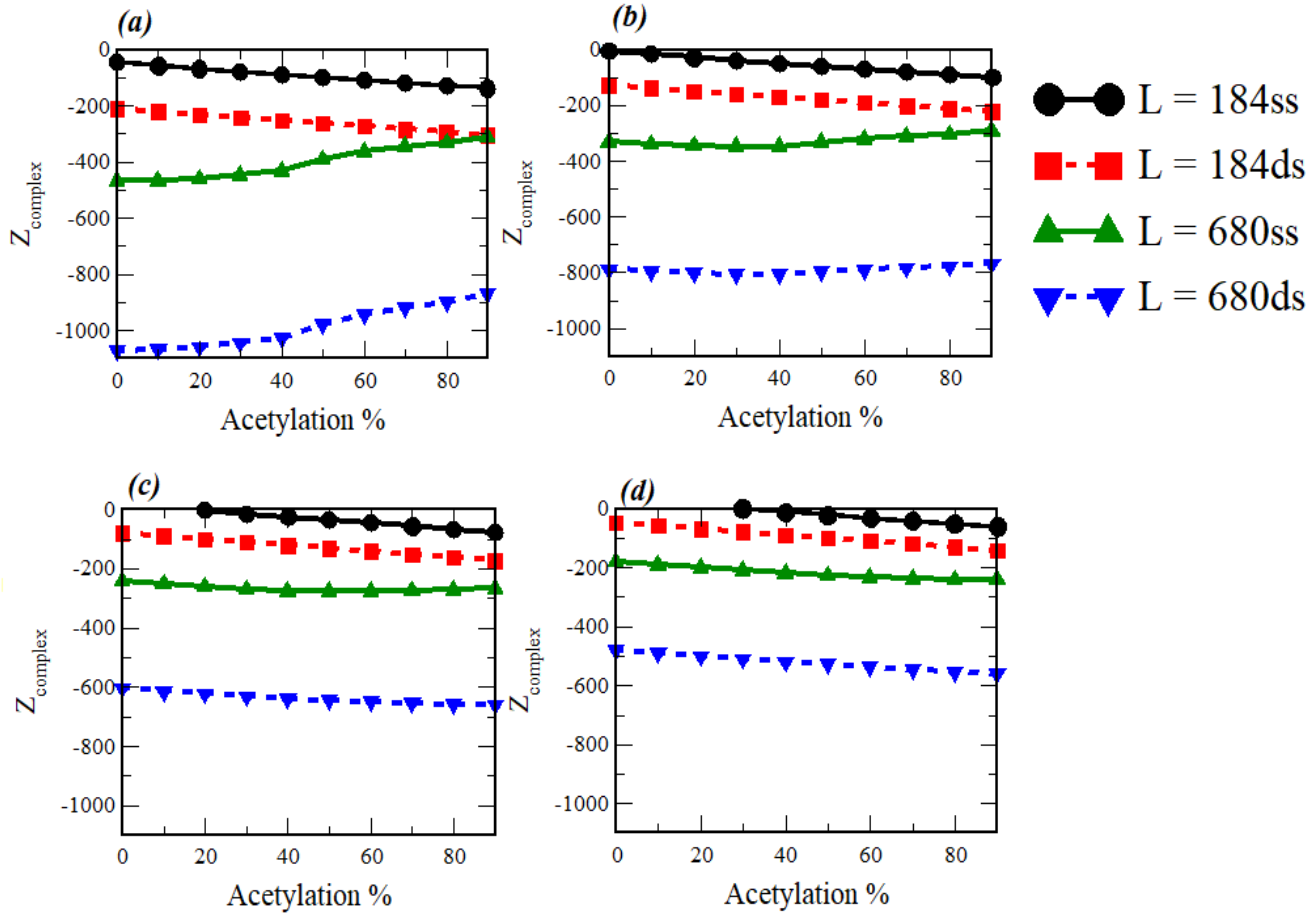

Figure 3.11: The net charge of the complex Z^* ($Z_{complex}$) as a function of acetylation %. (a) for N=3, (b) for N=4, (c) for N=5, and (d) for N=6. When L = 184 nm and L = 680 nm. Solid lines for ss chains, and dashed lines for ds chains.

The number of turns of PE wrapping around dendrimers with more than two dendrimers reaching to six dendrimers is illustrated in Fig. (3.12), and from this figure, the number of turns is slightly

constant for complexes using a length of 184 nm when using N = 3 to 6, in the case of ss and ds chains, by increasing acetylation. While for complexes using a length of 680 nm, a small increase in the number of turns was found by increasing acetylation when using N = 3 and N = 4 above 40% acetylation in the case of the ss chain. While being slightly fixed by increasing acetylation in the case of the ds chain. Furthermore, complexes with dendrimer numbers of N = 5 and 6 have a fixed number of turns wrapping around these dendrimers in the case of ss and ds chains.

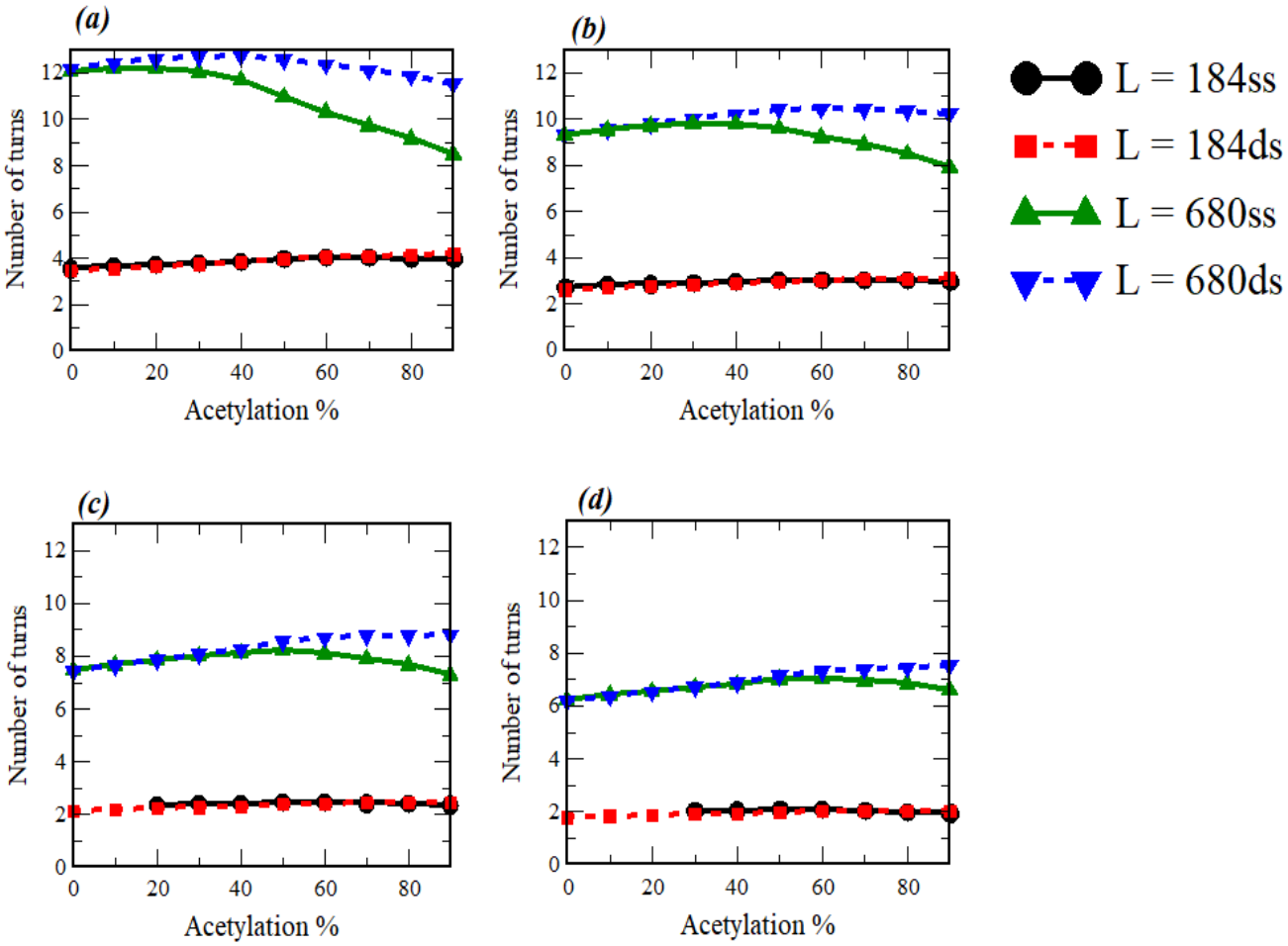

Figure 3.12: Number of turns of LPE chain on the dendrimer as a function of acetylation %. (a) for N=3, (b) for N=4, (c) for N=5, and (d) for N=6. When L = 184 nm and L = 680 nm. Solid lines for ss chains, and dashed lines for ds chains.

The number of turns wrapping around a dendrimer for complexes using a chain length of 680 nm in the case of ds, and a number of dendrimers ranging from 2 to 6 is illustrated in three-dimensional images at 0%, 40%, and 90% acetylation in Figs. (3.13), (3.14) and (3.15), respectively.

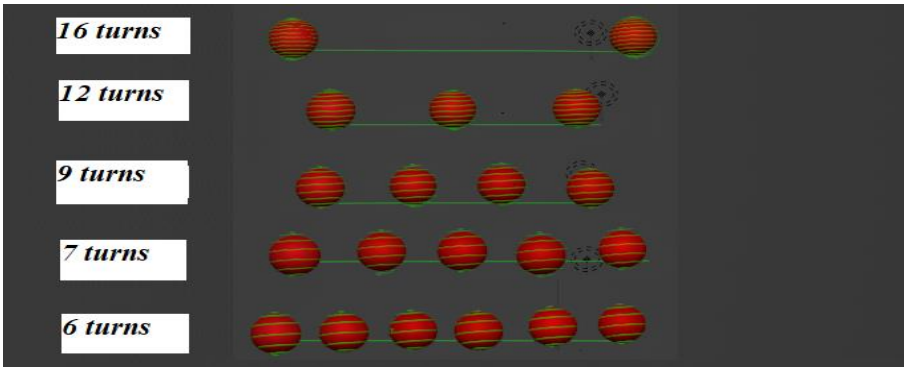

Figure 3.13: Number of turns of LPE chain on the dendrimer at zero % acetylation, when N=2, 3, 4, 5, and 6 and L=680 nm as a ds chain.

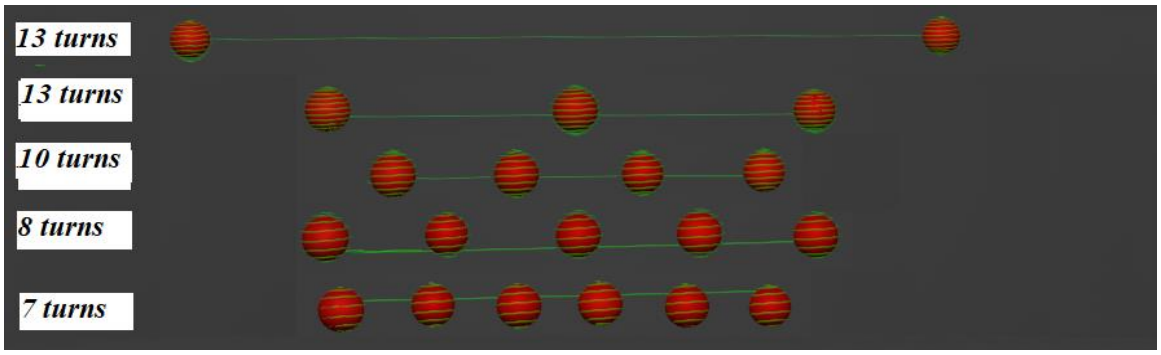

Figure 3.14: Number of turns of LPE chain on the dendrimer at 40 % acetylation, when N=2, 3, 4, 5, and 6 and L=680 nm as a ds chain.

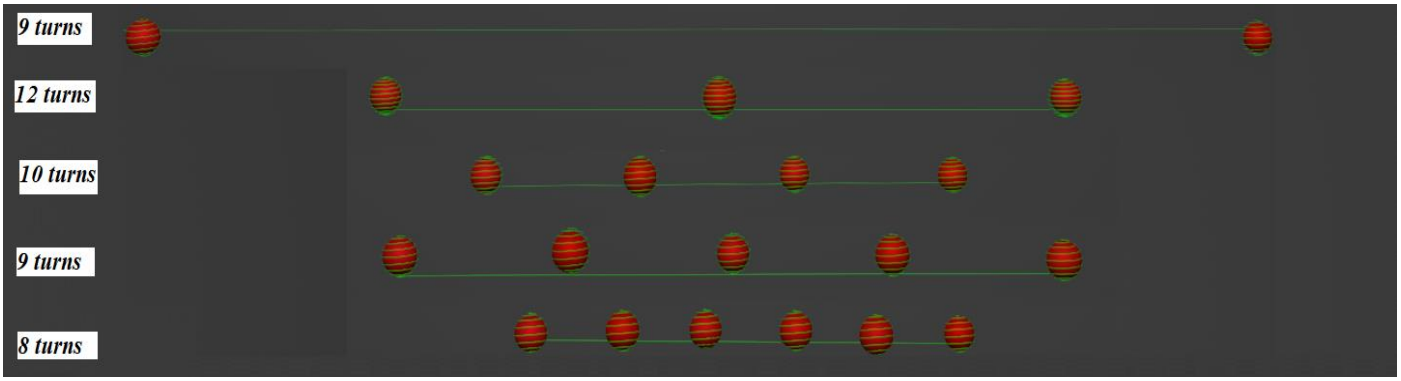

Figure 3.15: Number of turns of LPE chain on the dendrimer at 90 % acetylation, when N=2, 3, 4, 5, and 6 and L=680 nm as a ds chain.

3.4.2 Effect of LPE chain length on the zero acetylated dendrimer - LPE complex.

The effect of LPE chain length on the optimal length wrapping around dendrimer N and on the linker formed between complexes has been studied. The system is composed of G5 PAMAM dendrimers N=1,2,3,4,5, and 6 with charges Z_d of 128 and 96 and a R_s of 2.67 nm and 5.3 nm for the EDA and ammonia cores, respectively, at zero acetylation. The flexible LPE chain used has a l_p of 3 nm at a 1:1 salt concentration, which corresponds to a DSL of 100 nm. A b of 0.7 nm and a Bjerum length of 0.71 nm were used.

Fig. (3.16) illustrates that the length of the polyelectrolyte affects the l_{opt} and the linker created between the complexes. It demonstrates that as the length of the polyelectrolyte grows, the l_{opt} increases, as found by Shklovskii's N-spheres model (Nguyen and Shklovskii, 2001). As a result, the linker increases significantly, as shown in Fig. (3.16) (b), and the observations are consistent with the simulation results from Larin (Larin et al., 2010). Additionally, because the radius of a dendrimer with an ammonia core is larger, it has a lower curvature and a higher surface charge density, allowing the neutralization to be more successful. Whereas a dendrimer with an EDA core has a larger curvature and lower surface charge density, which reduces the effectiveness of the neutralization. As a result, and in agreement with Qamhieh and co-workers' results, the l_{opt} around the dendrimer will increase as the dendrimer's size increases (Qamhieh et al., 2014). Also, due to

the larger radius size of the dendrimer with an ammonia core, it requires less elastic (bending) energy for condensation compared to the dendrimer with an EDA core, which requires more elastic (bending) energy to allow the wrapping of PE around the dendrimer (Eq, 3). Moreover, we can see from this figure that as the number of dendrimers N increases, the l_{opt} wrapping around them will shorten, as revealed in Qamhieh and coworkers' studies (Qamhieh et al., 2009). They show that the l_{opt} wrapped around the dendrimer particles with the higher N is shorter than the l_{opt} wrapped around the dendrimer particles with the lower N. Furthermore, the l_{opt} wrapping around the dendrimer with an ammonia core was longer than that for the dendrimer with an EDA core. As a result, the linker length for the dendrimers with an ammonia core was significantly shorter than the linker length for the dendrimers with an EDA core, as shown in fig. (3.16) (b). We credit the reduction in the linker between complexes for the increase in the l_{opt} wrapped around the dendrimer. The complex's positive charge is decreased, and as a result, the complexes' repulsive electrostatic interaction is diminished as well.

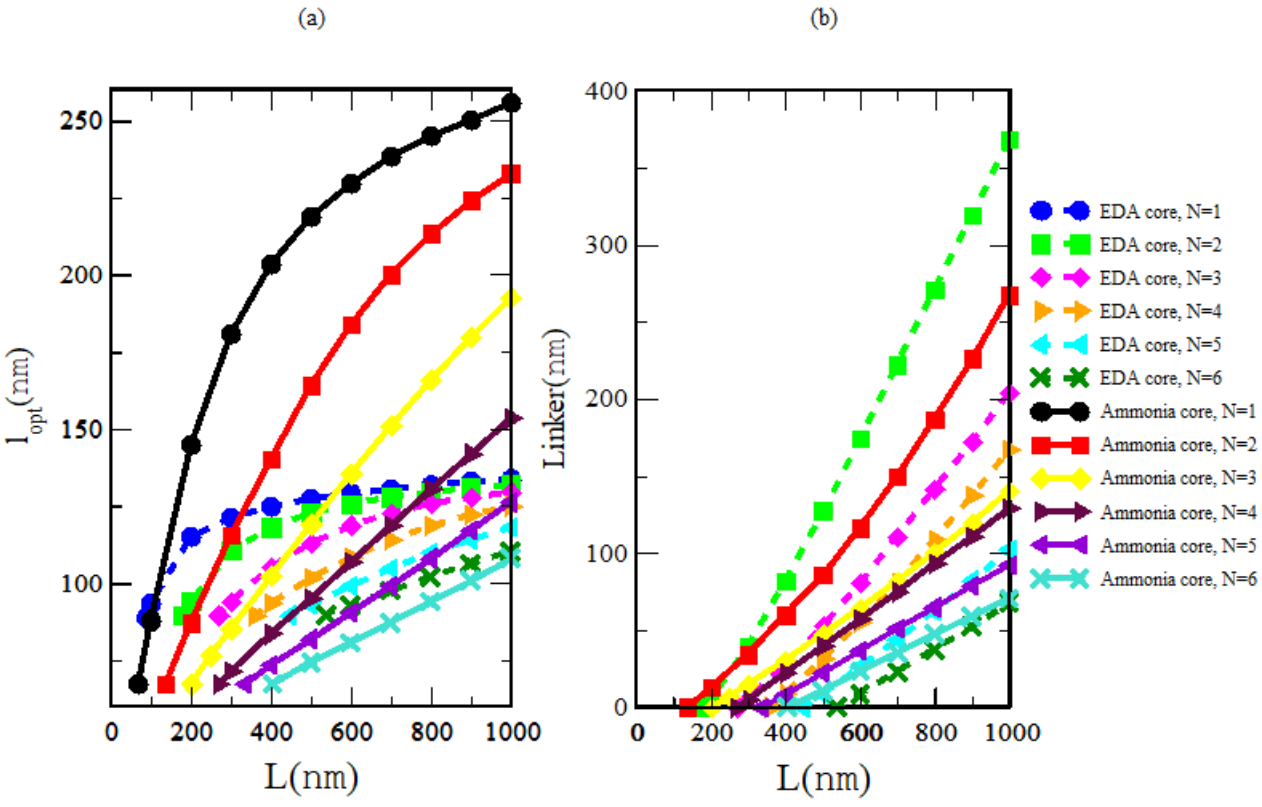

Figure 3.16: l_{opt} and Linker formed between G5 complexes with an oppositely charged flexible

LPE as a function of chain length L. (a) For optimal length, (b) for linker formed between G5 complexes. Dashed lines for EDA core and solid lines for ammonia core.

Numerous factors that are discussed below had an impact on these outcomes. First, the PE chain's length L, the next, number of dendrimer particles N used in the system, and lastly, the radius of each dendrimer. Additionally, these findings match the expectations of Qamhieh et al., 2022; Qamhieh et al., 2014; and Larin et al., 2010).

Fig. (3.17) demonstrates that by increasing the PE chain length, the ratio of l_{opt} wrapping around dendrimer with EDA and ammonia cores to the PE chain length decreases noticeably. An important point that we should pay attention to is N. This means that the degree of l_{opt} wrapping around the dendrimer is highest when there is only one particle, and as the N increases, the degree of l_{opt} wrapping around the dendrimer will decrease due to the formation of linkers between complexes, which means that a fraction of the PE chain will form between these dendrimers rather than around them. Also, when using shorter chain lengths, the l_{opt} starts to wrap earlier for complexes using one dendrimer. To be more precise, the l_{opt} starts to wrap around dendrimer with an ammonia core with a shorter chain length of 68 nm, and for dendrimer with an EDA core, the l_{opt} starts to wrap with a longer chain length of 90 nm. This is because the dendrimer with an ammonia core has a larger radius size, which has lower elastic (bending) energy than that of a smaller dendrimer radius size, while the dendrimer with an EDA core, which has a smaller radius size, needs more elastic (bending) energy to allow the l_{opt} to wrap around it (Eq, 3).

Furthermore, the neutralization of a dendrimer with an EDA core with the PE chain will be less efficient since the EDA core has a larger curvature and lower surface charge density, which reduces neutralization, whereas the ammonia core has a lower curvature and a higher surface charge density, as proved by Qamhieh et al. (2014). They discovered that G2's low surface charge density made neutralization less efficient than for G6 and G8, which had better neutralization that improved bending with the negatively charged DNA.

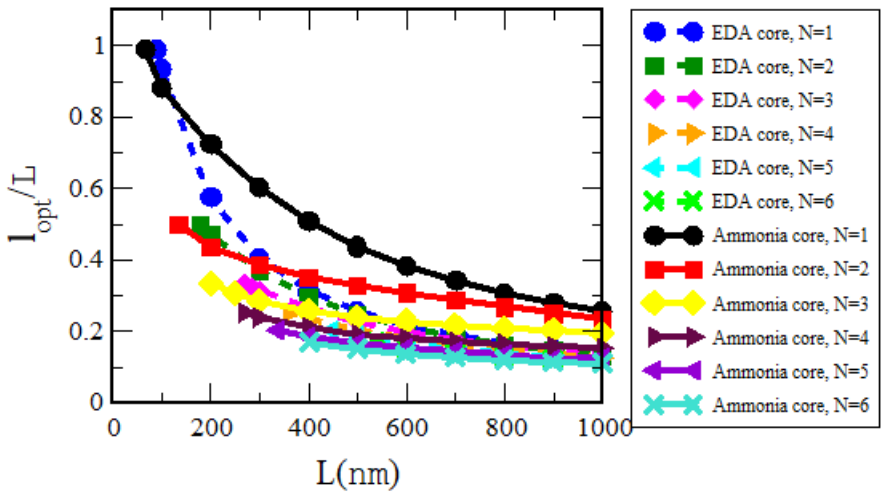

Figure 3.17: The ratio of l_{opt} to the length of PE as a function of PE chain length L. For EDA core (dashed lines), for ammonia core (solid lines).

Fig. (3.18) illustrates the condensed monomers of LPE on dendrimers using the penetrable sphere model for different LPE chain lengths, which are estimated theoretically. These results were compared with the expectations of the Qamhieh and co-workers (Qamhieh et al., 2009; Qamhieh et al., 2014; Qamhieh et al.,2022), Shklovskii model (Nguyen and Shklovskii, 2001) and BD simulations (Lyulin, 2005).

(a) demonstrates that, as discovered by Lyulin et al. (2005), increasing the chain length L considerably increases the number of condensed monomers on the dendrimer. Additionally, it shows that the dendrimer with the ammonia core has more condensed monomers, and it starts to interact with it at lower degrees and when using shorter chain lengths than the dendrimer with the EDA core. This is because the dendrimer with the ammonia core has a lower curvature and a larger surface charge density. As a result, they can interact with DNA charges more successfully. These results support those of Qamhieh et al. (2014).

Furthermore, due to the larger radius size of the dendrimer with an ammonia core, it requires less elastic (bending) energy for condensation compared to the dendrimer with an EDA core, which requires more elastic (bending) energy to allow the condensation of monomers around the dendrimer (Eq, 3). Also, an important point that we should pay attention to is that the number of condensed monomers on the dendrimer is highest when there is only one particle, and as N increases, the

number of condensed monomers on the dendrimer will decrease due to the formation of linkers between complexes, which means that some of these monomers will be consumed in the formation of linkers between these dendrimers rather than condensing on them.

(b) demonstrates that increasing the chain length results in more turns being wrapped around the dendrimer, which is consistent with the findings of Qamhieh and coworkers (Qamhieh et al., 2009). Additionally, it shows that the number of turns wrapping around the dendrimer with an EDA core, which has a smaller radius and circumference, is greater than the number of turns wrapping around the dendrimer with an ammonia core, which has a larger radius and circumference, in accordance with Qamhieh and coworkers' findings (Qamhieh et al., 2009). They studied the interaction between G4 dendrimers and the shorter DNA (2000 bp), and they discovered that much more turns were made around the dendrimer when the dendrimer's radius was reduced.

Moreover, the number of turns around ammonia core dendrimers begins to appear and wrap at lower degrees than dendrimers with an EDA core. Also, it starts to appear and wrap when using shorter chain lengths. These results happen for the same reasons discussed in Fig. (a) and Fig. (b) (Eq.3). When comparing these findings to earlier research on penetrable spheres by Qamhieh et al. (2009), who used a different type of dendrimer, and to the work by Arcesi et al. (2007), they all conclude that more turns will wrap around the smaller dendrimer radius. Also, as the number of dendrimer N increases, the number of turns wrapping around these dendrimers decreases. This is in agreement with research by Qamhieh and colleagues (Qamhieh et al., 2009), who examined the complexation between G4 dendrimers and DNA for two different DNA contour lengths and discovered that the number of turns was lower for the system that used multiple dendrimers.

The creation of linkers between complexes, which implies that a part of the PE chain will form between these dendrimers rather than around them, is another reason why the number of turns around the dendrimer decreases as the number of dendrimer particles bonded with it increases. This is in line with what Qamhieh and coworkers reported, as well as what Larin et al. revealed in their simulation research (Qamhieh et al., 2022; Larin et al., 2010).

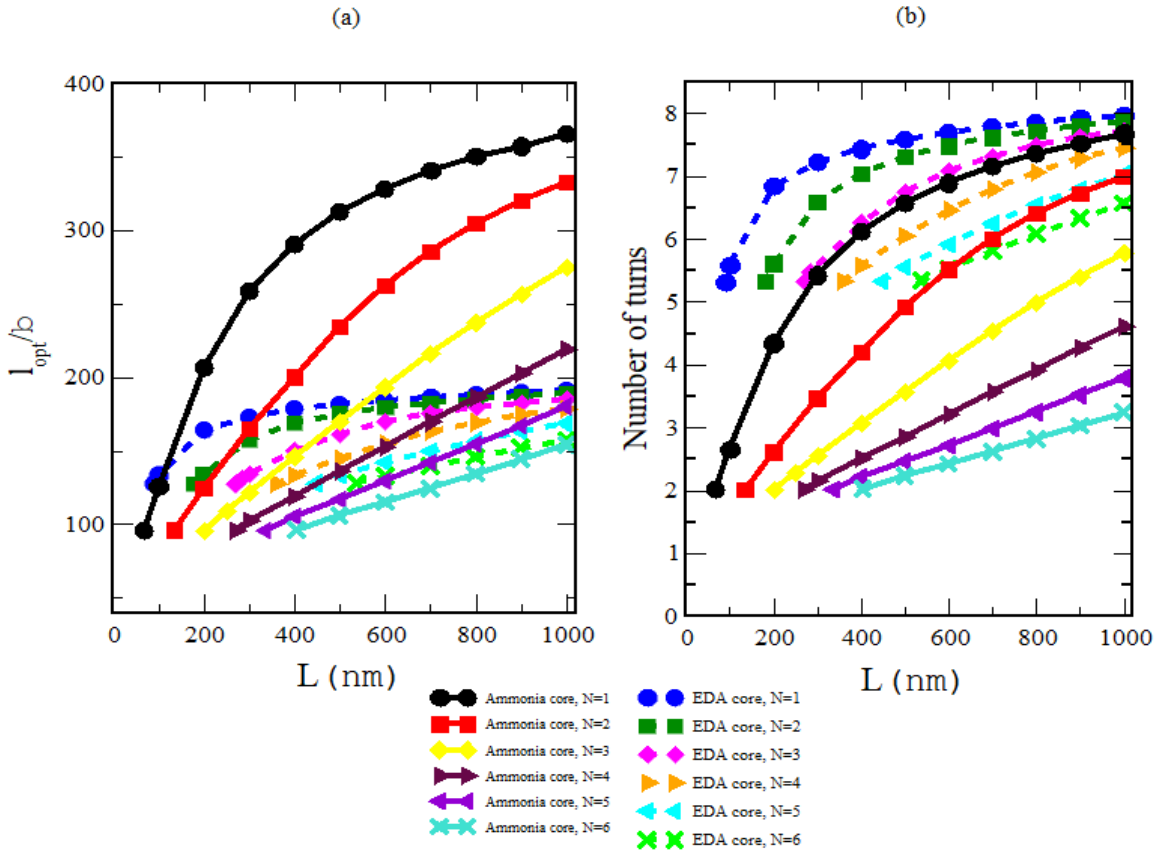

Figure 3.18: (a)The number of condensed monomers as a function of PE chain length (b) the number of turns warp around dendrimer as a function of PE chain length L. Dashed lines for EDA core, and solid lines for ammonia core.

Chapter Four

Conclusions

The theoretical study that we have provided here is the first theoretical investigation that has accounted for the interaction of a flexible and semiflexible polyelectrolyte as a model of DNA with an oppositely acetylated penetrable charged sphere (dendrimer). The acetylation decreases the size and charge of of G5 dendrimers, which in turn affects the resulting complex structure of the dendrimer and the LPE chain. We have demonstrated that as the acetylation percentage increases, the ratio of optimal wrapping length to the chain length and the number of condensed monomers around the dendrimer decrease for all the chain lengths used; 90, 184, and 680 nm in the case of using single dendrimer. Also, we studied the complexation of PE with multiple dendrimers; our results reveal that by increasing the acetylation percentage, the optimal length decreases and the linker increases. Our findings are in strong accordance with those of Qamhieh's earlier investigations.

In addition, we studied the properties of two systems; one composed of a semi-flexible LPE chain with one dendrimer, and the other with two dendrimers. We found out that the optimal length is larger than the isoelectric length, which requires compensating the total charge of the dendrimer when the dendrimer size is shrunk, which means that charge inversion for the dendrimer occurred. This result matches the simulation study carried out by Lyulin et al. (2005) and a theoretical study performed by Qamhieh et al. (2009). However, by increasing the acetylation %, the optimal length of all used lengths decreases significantly. The number of turns of ssDNA and dsDNA chains of 90 and 184 nm around the acetylated dendrimer was roughly constant with increasing acetylation %, while the number of turns of ssDNA and dsDNA chains with a length of 680 nm around the dendrimer dramatically decreased. These two systems differ in the complex net charge, for PE – single dendrimer, the complexes with lengths of 90 nm for both ssDNA and dsDNA, have negative net charges, which get more negative as R_s decreases. For lengths of 184 nm from 30% to 100% acetylation, and 680 nm, from 0% to 90% acetylation, in both cases of ssDNA and dsDNA, the net charge is negative and decrease in negativity. For PE – two dendrimer complexes. the net charge of the complexes with lengths of 90 and 184 nm of both ssDNA and dsDNA is negative and increases in negativity by decreasing R_s. For the complexes, using a length of 680 nm in the case of ssDNA

and dsDNA, it was shown that the net charge of the complexes decreased in its negative charge by decreasing R_s.

We studied the flexible PE-dendrimer complexes at zero acetylation. We found that by increasing the chain length, the ratio of optimal wrapping length to the chain length decreased significantly, while the optimal length, the linker length, the condensed monomers, and the number of turns were increased. This effect happens with an ammonia and EDA cores dendrimers, with a small variation in value due to the differences in charge and radius from one core to another. Moreover, at different acetylation percentages, we also investigated the complexes formed between semiflexible LPE chain with multiple dendrimers, which range from two to six. Our research has led us to conclude that as the optimal length decreases, the linker increases by increasing acetylation.

Most of these findings are inconsistent with other theoretical studies of; Netz and Joanny 1999, Nguyen and Shklovskii 2001, Qamhieh et al. 2009, and Qamhieh et al. 2014, in addition to computer simulations of; Luylin et al. 2005, Larin et al. 2010, and Nandy and Maiti 2011. However, the current global analytical work has significant practical implications and appears to be an inspiring topic for future gene therapy research. We expect that newly created model will be able to produce greater outcomes. Despite this, small improvements might be made to the established model in order to examine different types of LPEs with new various lengths greater than 680 nm, and to examine multi-spheres with more than N = 6. Furthermore, it is possible to introduce new variables to obtain more useful data, such as through studying other types of dendrimers.

References

1. Abu Abed, O. S. (2021): Gene therapy avenues and COVID-19 vaccines. Genes & Immunity, 22(2), 120-124.
2. Ainalem, M. L., & Nylander, T. (2011): DNA condensation using cationic dendrimers—morphology and supramolecular structure of formed aggregates. *Soft Matter*, *7*(10), 4577-4594.
3. An, M. (2016): Understanding DNA Condensation by Low Generation (G0/G1) and Zwitterionic G4 PAMAM Dendrimers. University of Kentucky, Lexington.
4. Arcesi, L., Penna, G. L., & Perico, A. (2007): Generalized electrostatic model of the wrapping of DNA around oppositely charged proteins. *Biopolymers: Original Research on Biomolecules*, *86*(2), 127-135.
5. Bae, S., Oh, I., Yoo, J., & Kim, J. S. (2021): Effect of DNA Flexibility on Complex Formation of a Cationic Nanoparticle with Double-Stranded DNA. *ACS omega*, *6*(29), 18728-18736.
6. Boas, U., Christensen, J. B., & Heegaard, P. M. (2006): Dendrimers in medicine and biotechnology: new molecular tools. Royal Society of Chemistry; pp. 1–27.
7. Brunet, A., Tardin, C., Salome, L., Rousseau, P., Destainville, N., & Manghi, M. (2015): Dependence of DNA persistence length on ionic strength of solutions with monovalent and divalent salts: a joint theory–experiment study. *Macromolecules*, *48*(11), 3641-3652.
8. Caetano, D. L., & de Carvalho, S. J. (2017): Conformational properties of block-polyampholytes adsorbed on charged cylindrical surfaces. *The European Physical Journal E*, *40*(3), 1-8.
9. Caetano, D. L., de Carvalho, S. J., Metzler, R., & Cherstvy, A. G. (2020): Critical adsorption of multiple polyelectrolytes onto a nanosphere: splitting the adsorption–desorption transition boundary. *Journal of the Royal Society Interface*, *17*(167), 20200199.
10. Caminade, A. M., Turrin, C. O., Laurent, R., Ouali, A., & Delavaux-Nicot, B. (Eds.). (2011): Dendrimers: towards catalytic, material and biomedical uses. John Wiley & Sons, Italy.

11. Chuang, H. M., Reifenberger, J. G., Cao, H., & Dorfman, K. D. (2017): Sequence-dependent persistence length of long DNA. *Physical review letters*, *119*(22), 227802.

12. Ciolkowski, M., Petersen, J. F., Ficker, M., Janaszewska, A., Christensen, J. B., Klajnert, B., & Bryszewska, M. (2012): Surface modification of PAMAM dendrimer improves its biocompatibility. Nanomedicine: Nanotechnology, Biology and Medicine, 8(6), 815-817.

13. De Carvalho, S. J., Metzler, R., & Cherstvy, A. G. (2014): Critical adsorption of polyelectrolytes onto charged Janus nanospheres. *Physical Chemistry Chemical Physics*, *16*(29), 15539-15550.

14. DNA - Wikipedia. (n.d.). DNA - Wikipedia. https://en.wikipedia.org/wiki/DNA.

15. Fant, K., Esbjörner, E. K., Jenkins, A., Grossel, M. C., Lincoln, P., & Nordén, B. (2010): Effects of PEGylation and acetylation of PAMAM dendrimers on DNA binding, cytotoxicity and in vitro transfection efficiency. Molecular pharmaceutics, 7(5), 1734-1746.

16. Fatemi, S. M., Fatemi, S. J., & Abbasi, Z. (2020): PAMAM dendrimer-based macromolecules and their potential applications: recent advances in theoretical studies. *Polymer Bulletin*, *77*(12), 6671-6691.

17. Fedorov. (2013). GetData Graph Digitizer. Get the software safely and easily. Software Informer. https://getdata-graph-digitizer.software.informer.com/.

18. Fox, L. J., Richardson, R. M., & Briscoe, W. H. (2018): PAMAM dendrimer-cell membrane interactions. *Advances in colloid and interface science*, *257*, 1-18.

19. Grayson, S. M., & Frechet, J. M. (2001): Convergent dendrons and dendrimers: from synthesis to applications. Chemical reviews, 101(12), 3819-3868.

20. Gupta, S., & Biswas, P. (2020): Conformational properties of complexes of poly (propylene imine) dendrimers with linear polyelectrolytes in dilute solutions. *The Journal of Chemical Physics*, *153*(19), 194902.

21. Huang, Y. C., Su, C. J., Chen, C. Y., Chen, H. L., Jeng, U. S., Berezhnoy, N. V., ... & Ivanov, V. A. (2016): Elucidating the DNA–Histone Interaction in Nucleosome from the DNA–Dendrimer Complex. *Macromolecules*, *49*(11), 4277-4285.

22. Humphrey, W., Dalke, A., & Schulten, K. (1996): VMD: visual molecular dynamics. *Journal of molecular graphics*, *14*(1), 33-38.

23. Janaszewska, A., Lazniewska, J., Trzepiński, P., Marcinkowska, M., & Klajnert-Maculewicz, B. (2019): Cytotoxicity of dendrimers. *Biomolecules*, *9*(8), 330.

24. Jevprasesphant, R., Penny, J., Jalal, R., Attwood, D., McKeown, N. B., & D'emanuele, A. (2003): The influence of surface modification on the cytotoxicity of PAMAM dendrimers. International journal of pharmaceutics, 252(1-2), 263-266.

25. Jin, Y. J., Luo, Y. J., Li, G. P., Li, J., Wang, Y. F., Yang, R. Q., & Lu, W. T. (2008): Application of photoluminescent CdS/PAMAM nanocomposites in fingerprint detection. *Forensic Science International*, *179*(1), 34-38.

26. Kolhatkar, R. B., Kitchens, K. M., Swaan, P. W., & Ghandehari, H. (2007): Surface acetylation of polyamidoamine (PAMAM) dendrimers decreases cytotoxicity while maintaining membrane permeability. *Bioconjugate chemistry*, *18*(6), 2054-2060.

27. Labieniec, M., & Watala, C. (2009): PAMAM dendrimers—Diverse biomedical applications. Facts and unresolved questions. *Central European Journal of Biology*, *4*(4), 434-451.

28. Larin, S. V., Lyulin, S. V., Darinskii, A. A., (2009): Charge Inversion of Dendrimers in Complexes with Linear Polyelectrolytes in the Solutions with Low pH Polymer Science, Ser. 51, 459– 468.

29. Larin, S.V., Darinskii, A. A., Lyulin, A. V., Lyulin, S. V., (2010): Linker Formation in an Overcharged Complex of Two Dendrimers and Linear Polyelectrolyte, J. Phys. Chem., 114, 2910-2919.

30. Lee, H., & Larson, R. G. (2006): Molecular dynamics simulations of PAMAM dendrimer-induced pore formation in DPPC bilayers with a coarse-grained model. *The journal of physical chemistry B*, *110*(37), 18204-18211.

31. Lee, H., & Larson, R. G. (2009): Multiscale modeling of dendrimers and their interactions with bilayers and polyelectrolytes. *Molecules*, *14*(1), 423-438.

32. Liu, Q., Shaukat, A., Kyllönen, D., & Kostiainen, M. A. (2021): Polyelectrolyte Encapsulation and Confinement within Protein Cage-Inspired Nanocompartments. *Pharmaceutics*, *13*(10), 1551.

33. Lyulin, S. V., Darinskii, A.A., Lyulin, A. V., (2005): Computer Simulation of Complexes of Dendrimers with Linear Polyelectrolytes, Macromolecules, 38, 3990-3998.

34. Lyulin, S.V., Vattulainen, L., Gurtovenko, A. A., (2008): Complexes Comprised of Charged Dendrimers, Linear Polyelectrolytes, and Counterions: Insight through Coarse-Grained Molecular Dynamics Simulations. Macromolecules, 41, 4961-4968.

35. Ma, Y. Q. (2013): Theoretical and computational studies of dendrimers as delivery vectors. *Chemical Society Reviews*, *42*(2), 705-727.

36. Maiti, P. K., & Bagchi, B. (2006): Structure and dynamics of DNA− dendrimer complexation: role of counterions, water, and base pair sequence. *Nano letters*, *6*(11), 2478-2485.

37. Maiti, P. K., Çağın, T., Lin, S. T., & Goddard, W. A. (2005); Effect of solvent and pH on the structure of PAMAM dendrimers. *Macromolecules*, *38*(3), 979-991.

38. Maiti, P. K., Çağın, T., Wang, G., & Goddard, W. A. (2004): Structure of PAMAM dendrimers: Generations 1 through 11. *Macromolecules*, *37*(16), 6236-6254.

39. Malik, N., Wiwattanapatapee, R., Klopsch, R., Lorenz, K., Frey, H., Weener, J. W., & Duncan, R. (2000): Dendrimers: Relationship between structure and biocompatibility in vitro, and preliminary studies on the biodistribution of 125I-labelled polyamidoamine dendrimers in vivo. Journal of Controlled Release, 65(1-2), 133-148.

40. Maysinger, D., Zhang, Q., & Kakkar, A. (2020): Dendrimers as Modulators of Brain Cells. *Molecules*, *25*(19), 4489.

41. Mecke, A., Lee, D. K., Ramamoorthy, A., Orr, B. G., & Banaszak Holl, M. M. (2005): Synthetic and natural polycationic polymer nanoparticles interact selectively with fluid-phase domains of DMPC lipid bilayers. *Langmuir*, *21*(19), 8588-8590.

42. Meka, V. S., Sing, M. K., Pichika, M. R., Nali, S. R., Kolapalli, V. R., & Kesharwani, P. (2017): A comprehensive review on polyelectrolyte complexes. *Drug discovery today*, *22*(11), 1697-1706.

43. Müller, M. (2013): *Polyelectrolyte complexes in the dispersed and solid state II* (Vol. 256). Springer, Berlin.

44. Nandy B, Maiti PK (2010): DNA compaction by a dendrimer. J Phys Chem B 115:217–230

45. Netz, R. R., & Joanny, J. F. (1999): Adsorption of semiflexible polyelectrolytes on charged planar surfaces: charge compensation, charge reversal, and multilayer formation. *Macromolecules*, *32*(26), 9013-9025.

46. Netz, R. R., & Joanny, J. F. (1999): Complexation between a semiflexible polyelectrolyte and an oppositely charged sphere. *Macromolecules*, *32*(26), 9026-9040.

47. Nguyen, T. T., & Shklovskii, B. I. (2001): Overcharging of a macroion by an oppositely charged polyelectrolyte. *Physica A: Statistical Mechanics and its Applications*, *293*(3-4), 324-338.

48. Ohshima, H., & Kondo, T. (1993): Electrostatic double-layer interaction between two charged ion-penetrable spheres: an exactly solvable model. *Journal of colloid and interface science*, *155*(2), 499-505.

49. Palmerston Mendes, L., Pan, J., & Torchilin, V. P. (2017): Dendrimers as nanocarriers for nucleic acid and drug delivery in cancer therapy. Molecules, 22(9), 1401.

50. PAMAM Dendrimers. (2018): PAMAM Dendrimers. Retrieved December 1, 2022, from https://www.dendritech.com/pamam.htm.

51. Papagiannopoulos, A. (2021): Current Research on Polyelectrolyte Nanostructures: From Molecular Interactions to Biomedical Applications. *Macromol*, *1*(2), 155-172.

52. Parat, A., & Felder-Flesch, D. (2016): General introduction on dendrimers, classical versus accelerated syntheses and characterizations. In Dendrimers in Nanomedicine. Jenny Stanford Publishing. 1-22.

53. Pereyra, A., & Hereñu, C. (2013). Gene delivery systems. In Current issues in molecular virology—viral genetics and biotechnological applications. Rijeka: INTECH.

54. Peters, J. P., & Maher, L. J. (2010): DNA curvature and flexibility in vitro and in vivo. Quarterly reviews of biophysics, 43(1), 23-63.

55. Qamhieh, K., & Khaleel, A. A. (2014): Analytical model study of complexation of dendrimer as an ion penetrable sphere with DNA. *Colloids and Surfaces A: Physicochemical and Engineering Aspects*, *442*, 191-198.

56. Qamhieh, K., Nylander, T., Black, C. F., Attard, G. S., Dias, R. S., & Ainalem, M. L. (2014): Complexes formed between DNA and poly (amido amine) dendrimers of different generations–modelling DNA wrapping and penetration. *Physical Chemistry Chemical Physics, 16*(26), 13112-13122.

57. Rawat, K., Pathak, J., & Bohidar, H. B. (2013): Effect of persistence length on binding of DNA to polyions and overcharging of their intermolecular complexes in aqueous and in 1-methyl-3-octyl imidazolium chloride ionic liquid solutions. *Physical Chemistry Chemical Physics, 15*(29), 12262-12273.

58. Santos, A., Veiga, F., & Figueiras, A. (2019): Dendrimers as pharmaceutical excipients: synthesis, properties, toxicity and biomedical applications. *Materials, 13*(1), 65.

59. Scheller, E. L., & Krebsbach, P. H. (2009): Gene therapy: design and prospects for craniofacial regeneration. Journal of dental research, 88(7), 585-596.

60. Schiessel, H., (2003): The physics of chromatin, J. Phys.: Condens. Matter, 15, R699-R774.

61. Schiessel, H., Bruinsma, R. F., & Gelbart, W. M. (2001): Electrostatic complexation of spheres and chains under elastic stress. *The Journal of Chemical Physics*, *115*(15), 7245-7252.

62. Shi, L., Carn, F., Boué, F., & Buhler, E. (2016): Role of the ratio of biopolyelectrolyte persistence length to nanoparticle size in the structural tuning of electrostatic complexes. *Physical Review E, 94*(3), 032504.

63. Shifrina, Z. B., Kuchkina, N. V., Rutkevich, P. N., Vlasik, T. N., Sushko, A. D., & Izumrudov, V. A. (2009): Water-soluble cationic aromatic dendrimers and their complexation with DNA. *Macromolecules, 42*(24), 9548-9560.

64. Smith, P. E., Brender, J. R., Dürr, U. H., Xu, J., Mullen, D. G., Banaszak Holl, M. M., & Ramamoorthy, A. (2010): Solid-state NMR reveals the hydrophobic-core location of poly (amidoamine) dendrimers in biomembranes. *Journal of the American Chemical Society, 132*(23), 8087-8097.

65. Thinley, P. (2010): Technical comments on the design and designation of biological corridors in Bhutan: global to national perspectives. *Journal of Renewable Natural Resources, Bhutan, 6*, 91-106.

66. Waite, C. L., Sparks, S. M., Uhrich, K. E., & Roth, C. M. (2009): Acetylation of PAMAM dendrimers for cellular delivery of siRNA. *BMC biotechnology*, *9*(1), 1-10.

67. Welch, P., & Muthukumar, M. (2000): Dendrimer− Polyelectrolyte Complexation: A Model Guest− Host System. *Macromolecules*, *33*(16), 6159-6167.

68. What is DNA?: MedlinePlus Genetics. (n.d.). What Is DNA?: MedlinePlus Genetics. https://medlineplus.gov/genetics/understanding/basics/dna/.

69. Winter. (2017, February 5): QtGrace - Browse Files at SourceForge.net. QtGrace - Browse Files at SourceForge.net. https://sourceforge.net/projects/qtgrace/files/.

70. Wolski, P., & Panczyk, T. (2019): Conformational properties of PAMAM dendrimers adsorbed on the gold surface studied by molecular dynamics simulation. *The Journal of Physical Chemistry C*, *123*(36), 22603-22613.

71. Yu, S. (2015): *Experimental and Theoretical Studies of DNA-Macroion Interactions* (Doctoral dissertation).

72. Yu, S., Li, M. H., Choi, S. K., Baker, J. R., & Larson, R. G. (2013): DNA condensation by partially acetylated poly (amido amine) dendrimers: effects of dendrimer charge density on complex formation. *Molecules*, *18*(9), 10707-10720.

المركبات المتكونة بين البولي اليكترولايت وديندريمرات موجبة الشحنة تعرضت للأسيتيليشن.

اعداد: رغد عبد المعز داوود نتشه

المشرف: د. خولة قمحية

الملخص

لقد تمت دراسة نموذج نظري جديد استنادا على نتائج سابقة، بحيث يتم استخدام نوع من أنواع البوليمرات يسمى بالديندريمر على اعتباره كرة قابلة للإختراق من قبل الأيونات المحيطة به بحيث يتفاعل بدوره مع نموذج للحمض النووي يسمى بال (LPE chain). يكون هذا الديندريمر معرض لعامل خارجي بحيث يتم وضعه بمحلول يحتوي على مجموعات الأسيتل وتسمى هذه العملية بال (**acetylation**)، مما يؤدي الى انكماش هذا الديندريمر بحيث يقل التنافر الناتج عن الشحنة الموجبة لتفرعات الديندريمر من خلال تفاعلها مع شحنات سالبة من مجموعات الاسيتيل ما يسمى بال (**overcharging**). مما ادى الى نقصان في قطر الديندريمر وشحنته وهذا ما تم استخدامه لبناء نتائج جديدة.

لقد وجد أن مع زيادة نسبة ال **acetylation** وبالتالي نقصان قطر الديندريمر وشحنته فإن الجزء الملتف حول الديندريمر يقل وبالتالي عدد الشحنات السالبة (**condensed monomers**) لل **LPE chain** حول الديندريمر ستقل أيضا.

في حال كانت نسبة ال **acetylation** صفر بالمئة، تمت دراسة تأثير طول ال (**LPE chain** المرن)على شكل وارتباط هذا المركب المكون من الديندريمر وال **LPE chain** بحيث أن طول الجزء الملتف وعدد الشحنات السالبة وأيضا درجة الإلتفاف لل **LPE chain** حول الديندريمر تأثرت بزيادة طول ال **LPE chain**. بداية، نسبة الجزء الملتف حول الديندريمرإلى طول ال **LPE chain** ستقل، أما بالنسبة لعدد الشحنات السالبة ودرجة الإلتفاف لل **LPE chain** كلاهما سيزداد مع زيادة طول ال **LPE chain.** وتم إيجاد أن مع زيادة ال **LPE chain** فإن الجزء الملتف حول الديندريمر سيزيد وبالتالي زيادة في طول الجزء من ال **LPE chain** الذي يربط بين كرتين أو أكثرمن الديندريمر ما يسمى ب ال(**linker**).

بالإضافة إلى ذلك، تمت دراسة تأثير نسب مختلفة من ال **acetylation** على المركب المكون من ديندريمر و (**LPE chain** صلب) على الجزء الملتف حول الديندريمر وعلى الجزء الذي يربط بين عدة ديندريمرات، حيث وجد أن طول الجزء الملتف حول الديندريمر سيقل مع زيادة نسبة ال **acetylation** وبالتالي زيادة في طول جزء ال **LPE chain** الذي يربط بين كل كرتين أو أكثر من الديندريمر(**linker**).